Reparative dentin formation by dentin matrix proteins and small extracellular vesicles

Bo Wen, Yibing Huang, Tao Qiu, Fangjun Huo, Li Xie, Li Liao, Weidong Tian, Weihua Guo

PII: S0099-2399(20)30923-7

DOI: https://doi.org/10.1016/j.joen.2020.11.017

Reference: JOEN 4738

To appear in: *Journal of Endodontics*

Received Date: 18 August 2020

Revised Date: 30 October 2020

Accepted Date: 13 November 2020

Please cite this article as: Wen B, Huang Y, Qiu T, Huo F, Xie L, Liao L, Tian W, Guo W, Reparative dentin formation by dentin matrix proteins and small extracellular vesicles, *Journal of Endodontics* (2020), doi: https://doi.org/10.1016/j.joen.2020.11.017.

Reparative dentin formation by dentin matrix proteins and small extracellular vesicles

Bo Wen[1, 2, 3, 4], Yibing Huang[1, 2, 3, 4], Tao Qiu[1, 2, 3, 4], Fangjun Huo[1, 2, 3], Li Xie[1, 2, 3], Li Liao[1, 2, 3], Weidong Tian[1, 2, 3, 5*], Weihua Guo[1, 2, 3, 4*]

[1.] Engineering Research Center of Oral Translational Medicine, Ministry of Education, West China Hospital of Stomatology, Sichuan University, Chengdu, China

[2.] National Engineering Laboratory for Oral Regenerative Medicine, West China Hospital of Stomatology, Sichuan University, Chengdu, China

[3.] State Key Laboratory of Oral Diseases, National Clinical Research Center for Oral Diseases, West China Hospital of Stomatology, Sichuan University, Chengdu, China

[4.] Department of Pediatric Dentistry, West China Hospital of Stomatology, Sichuan University, Chengdu, China

[5.] Department of Oral and Maxillofacial Surgery, West China Hospital of Stomatology, Sichuan University, Chengdu, China University, Chengdu, China

* Corresponding authors at: Weihua Guo, Department of Pediatric Dentistry, West China School of Stomatology, Sichuan University, No. 14, 3rd Section, Ren Min Nan Road, Chengdu 610041, China. E-mail: guoweihua943019@163.com

* Corresponding authors at: Weidong Tian, Department of Oral and Maxillofacial Surgery, West China School of Stomatology, Sichuan University, No. 14, 3rd Section, Ren Min Nan Road, Chengdu 610041, China. E-mail: drtwd@sina.com

ACKNOWLEDGMENTS

This work is supported by the Sichuan Science and Technology Program (2017SZ0031), Nature Science Foundation of China (31470947, 31771062), National Key Technology R&D Program (2017YFA0104800).

The authors deny any conflicts of interest related to this study.

Reparative dentin formation by dentin matrix proteins and small extracellular vesicles

ABSTRACT

Introduction: Vital pulp therapy is aim at preserving pulp vitality and regenerating dentin. Therefore, the purpose of this study was to explore the effects of a combination of treated dentin matrix (TDM) proteins and dental pulp cell-derived small extracellular vesicle (sEV) on pulp-dentin complex repair. **Methods:** We prepared TDM by chemical demineralization and mechanical disruption of teeth to a powder preparation. The sEV were isolated from culture supernatants of dental pulp cells (DPCs) and identified by nanoparticle tracking analysis, western blotting, and transmission electron microscopy. The effect of a combination of TDM proteins and dental pulp cell-derived sEV on DPCs' proliferation, migration and odontogenic differentiation was evaluated *in vitro*. A mini-pig model of pulp injury was used to compare the clinical outcomes and tissue responses attributed to four materials including TDM, sEV-TDM, sEV and mineral trioxide aggregate (MTA). **Results:** The sEV isolated from the cell supernatant promoted DPCs proliferation and migration. The combination of TDM extracts and sEV synergistically promoted the migration of DPCs but suppressed their proliferation. RT-PCR and Western blot revealed that sEV-TDM enhanced the odontoblast related protein expressions in DPCs. *In vivo* studies, TDM and sEV-TDM promoted the formation of continuous reparative dentin. Furthermore, odontoblast-like high columnar cells were observed on the pulp side of the dentin bridge. **Conclusion:** The sEV-TDM complex exhibits intrinsic biological activities, which has potential applications as a bioactive pulp capping material.

KEYWORDS

Treated dentin matrix; Dental pulp cells; Extracellular vehicles; Vital pulp therapy

INTRODUCTION

Dental pulp tissue, as the only vascularized connective tissue in the teeth, plays a critical role in maintaining teeth stability and health. Damaged pulp tissue can significantly affect normal dental physiological functioning and survival[1]. Direct and indirect dental pulp therapy induces tertiary mineralized dentin secretion to prevent dental pulp necrosis, preserve the integrity, and prolong the lifetime of the tooth during the early stages of pulp infection in

young patients[2]. Recently, pulp capping materials such as calcium silicate-based cement (CSC) and calcium hydroxide (CH) have been utilized as natural tissue substitutes to mediate mineralized tissue formation by releasing Ca^{2+} and alkaline products[3]. The biological response of current pulp capping agents is considered to be a reparative process rather than a regeneration response. This is because it rarely catalyzes tissue regeneration to restore the dentin integrity and provide complete pulp defense[4].

Studies have reported the secretion of specific growth factors and bioactive molecules sequestered within the remaining dentin matrix contributes to the formation of reactionary dentin[5]. Current research confirmed that the treated dentin matrix (TDM), derived from dentin matrix, contains extracellular matrix components such as dentin sialoprotein (DSP), dentin matrix protein-1 (DMP-1), and transforming growth factor-β (TGF- β) that are associated with the occurrence, formation, and mineralization of dentin. When combined with dental follicle cells, TDM can be used to construct bio-root, as a dental implant replacement alternative for mission teeth[6-8]. *In vivo* and *in vitro*, research has shown that TDM, as mineralized dentin matrix proteins aggregates, exhibits superior bioactivity when compared to calcium hydroxide[9].

In case of pulp infection and/or traumatic injuries, dental pulp stem cells (DPSCs) in the primary and permanent teeth pulp are recruited to participate in the regeneration of the dentin-pulp tissue[10]. DPSCs can be differentiated into odontoblast-like cells and other cell lineages, such as osteoblasts and neuronal progenitor cells, which have been a promising tool for clinical applications in dental pulp regeneration[11]. But at present, stem cell therapy faces practical and regulatory obstacles such as donor matching, cell expansion and cryopreservation, which can restrict further research and wide clinical utility[12]. Accumulating evidence indicates that small extracellular vesicles (sEV) are considered being actively involved in intercellular functional activities associated with transfer mRNAs, miRNAs, and proteins transfer. It has been established that sEV play an important role in immunomodulation, cancer metastasis, and tissue regeneration[13]. Besides, mesenchymal stem cells (MSCs) derived sEV exhibit MSC-like characteristics and are involved in regenerative response regulation, which can be considered a capable induction unit to promote tissue regeneration as a promising cell-free bioactive molecule[14]. The sEV secreted

by DPSCs can promote odontoblast differentiation, attenuate neighboring cells apoptosis, exert a neuroprotective effect, and facilitate angiogenesis[15-17].

Based on preliminary research[6, 7, 9], the objective of this study was to determine the effects of dentin matrix proteins from TDM and sEV from DPCs on cell behavior of hDPCs including migration, proliferation and odontoblastic differentiation, and to explore the effect of TDM powder combined with sEV on exposed pulp tissue and dentin-pulp complex.

MATERIALS AND METHODS

Fabrication of TDM materials

Human TDM (hTDM) was prepared from routinely extracted healthy human third molars at the Oral Surgery Department of West China Hospital of Stomatology, Sichuan University School. The study was conducted in accordance with the guidelines of the Ethical Review Committee (Reference No. WCHSIRB-D-2017-134). An informed consent was obtained from all participants. Pig TDM (pTDM) was made from porcine incisors of 7-month-old pig jaws. The periodontium, periodontium, dental crown, dental pulp, and predentin of teeth were all removed by mechanical means using a high-speed handpiece (Dentsply Sirona, USA). The teeth were soaked in 17% ethylene diamine tetra-acetic acid (EDTA; Sigma, USA) for 30min, 10% EDTA for 30 min and 5% EDTA for 30 min, respectively. They were then cleaned with deionized water, and lyophilized, after which TDM was obtained and stored at −80 °C.

TDM was grounded into powder using a frozen grinding machine (MM400, Retsch, Germany) for 5 min at 30 Hz and examined by a scanning electron microscope (SEM, Inspect F, FEI, USA). The TDM powder (TDMP) with a diameter smaller than 40 μm were employed to get aqueous TDM extracts. Materials were sterilized by radiation of Co_{60} (Sichuan Institute of Atomic Energy, China). The extracts were obtained by introducing 1 g TDM in 5 ml α-MEM culture medium for 7 days[9]. Protein concentration in the TDM extracts was determined using the BCA method (keyGEN, China).

Cell culture of human DPCs

The extracted dental pulp tissues were sectioned into $1mm^3$ and digested with type I collagenase and dispase enzyme for 30 min[18]. The tissue fragments were transferred to sterile

α-minimal essential medium (α-MEM, Hyclone) containing 10% fetal bovine serum (FBS, Hyclone, USA) and 1% (v/v) penicillin/streptomycin solution (Hyclone, USA) at 37 □ in 5% CO_2 to obtain primary cells. The third-generation cells were used in later experiments. Cellular cytokeratin 14 (CK-14) and vimentin expression were analyzed by immunofluorescence staining following the manufacturer's protocol. Immunostaining was performed using primary antibodies against Vimentin (at 1:200 dilution, Santa Cruz, USA) and CK14 (a 1:200 dilution, Abcam, UK). Secondary antibodies including Alexa Fluor 488 (Goat anti Mouse at a 1:200 dilution, Invitrogen, USA), Alexa Fluor 555 (Goat anti Mouse at a 1:200 dilution, Invitrogen, USA) were used. After nuclei counterstained with DAPI reagent and the cells were examined under a fluorescence microscope (Leica Optical, Germany).

Identification of human DPCs

Several approaches such as osteogenic, adipogenic, and neurogenic differentiation have been used to characterize the stemness of hDPCs[6]. The hDPCs at a concentration of 1×10^5 were cultured separately in osteogenic, adipogenic, and neurogenic media for 21 days, 21 days, and 3 days. The osteogenic medium was supplemented with 10% FBS, 5 mM L-glycerophosphate (Sigma, USA), 100 nM dexamethasone (Sigma, USA), and 50 mg/ml ascorbic acid (Sigma, USA). The adipogenic medium was supplemented with 10% FBS, 2 mM insulin (Sigma, USA), 0.5 mM isobutylmethylxanthine (IBMX; Sigma, USA), and 10 nM dexamethasone (Sigma, USA). The neurogenic medium was supplemented with 2% DimethylSulphoxide (DMSO), 200 mM butylated hydroxyanisole (Sigma, USA), 25 mM KCl (Kelong, China), 2 mM valproic acid (Sigma, USA),10 mM forskolin (Sigma, USA), 1 mM hydrocortisone (Sigma, USA), 5 mg/mL insulin (Gibco, USA), and 2 mM L-glutamine (Sigma, USA). Cells in the control group were cultured in ordinary α-MEM supplemented with 10% FBS. After induction, the cells were stained with alizarin red solution (Sigma, USA) and Oil Red O solution (Sigma, USA) to assess their potential for osteogenic and adipogenic differentiation. Cells in the neurogenic medium were examined by immunofluorescent assay for Nestin (1:200, Abcam, USA) and analyzed under a fluorescence microscope (Leica Optical, Germany).

Flow cytometry was performed to determine the surface markers expression levels of hDPCs. The following antibodies were purchased from BD Life Sciences (BD, USA) and

used: CD29 (1:1000, PE), CD44 (1:1000, FITC), CD90 (1:1000, FITC), CD146 (1:1000, PE), CD166 (1:1000, PE), CD33 (1:1000, FITC), CD34 (1:1000, FITC), CD45 (1:1000, FITC). Flow cytometry analyses were performed on the Beckman Coulter Cytomics FC 500 MPL system (Beckman Coulter, USA).

The sEV isolation and identification

The sEV were isolated from the supernatants of cultured DPCs as detailed previously[19]. Briefly, DPCs at P3 generation were twice rinsed using PBS and cultured for 48h in α-MEM containing 10% exosome-depleted fetal bovine serum (SBI, USA). Cell culture medium supernatant was obtained, filtered using a 0.22-μm filter, and centrifuged at 1,200rpm for 30 min to eliminate cellular debris. Sterile supernatants were concentrated by centrifugation into Amicon® Ultra-50 Centrifugal Filter Units with Ultracel-3 membrane (3,000 Mw cut off membrane, Millipore, USA) at 5,000g for 30 min. The concentrate was mixed with the Total Exosome Isolation™ reagent (Life Technologies, USA) and incubated at 4 ℃ overnight. Thereafter, it was spun at 10,000 g for 1 h at 4 ℃. The resultant sEV-enriched fraction was re-suspended in 100 μl PBS and stored at -80 °C. The protein content of the isolated sEV was determined by the BCA method (keyGEN, China). For transmission electron microscopy, the sEV were fixed in 1% glutaraldehyde solution for 2h before the examination. Samples were loaded onto formvar carbon-coated grids and examined using a transmission electron microscope (TEM, Hitachi H7500, Japan) after negative staining with 1% aqueous phosphotungstic acid for 60s. For Nanoparticle tracking analysis (NTA), the sEV were diluted in PBS and analyzed using ZetaView® PMX 110 (Particle Metrix, Meerbusch, Germany). The markers of sEV, including CD63 (Zen Bioscience, China), heat shock protein70 (HSP 70, Zen Bioscience, China), and Alix (Zen Bioscience, China) were evaluated by Western blotting.

Endocytosis experiments of sEV.

To locate the vesicles，the DPCs-sEV were pre-treated with a membrane-labeling dye DiO (Invitrogen, USA) at 37℃ for 30min as previously described[20]. After precipitation with Total Exosome Isolation™ reagent (Life Technologies, USA), the vesicles were washed and resuspended in serum-free α-MEM. DPCs were seeded on confocal petri dishes and cocultured with DiO-labeled vesicles for 6h. The cells were then washed three times with

PBS, fixed in 4% paraformaldehyde, and stained with Phallotoxins (Invitrogen, USA). Finally, the stained cells were washed with PBS and imaged under a confocal microscope (Olympus FV1000, Japan).

Chemotaxis assay of hDPCs

Transwell chambers with 8 μm pore polycarbonate membranes (Corning, New York, NY, USA) were used to assess the migration ability of the cells. Briefly, hDPCs (1×10^4) were seeded into the upper chamber of the Transwell apparatus. TDM extracts with various hDPCs-sEV concentrations (0, 10, 50, 100, and 200 μg/mL) were placed in the lower chamber for 12 h. Cells were fixed with 4% paraformaldehyde for 30 min, stained with crystal violet for 20 min, and counted by NIH Image J software. All experiments were done in triplicates.

Determination of the proliferative capacity of hDPCs

The Cell Counting Kit-8 kit (Dojindo, Japan) was used to determine the effect of sEV-TDM on the proliferation of hDPCs. The hDPCs were seeded in 96-well plates at a density of 5×10^3 cells per well overnight. The cells were then maintained in leaching liquid of TDM containing different hDPCs-sEV concentrations (0, 10, 50, 100, and 200 μg/mL). The assay was performed following the manufacturer's instructions. The OD values were read on the Multiskan Go Spectrophotometer (Thermo Fisher Scientific, USA).

Quantitative Real-time Polymerase Chain Reaction (qRT-PCR)

The hDPCs were seeded at a concentration of 10^5 cells per well into six-well plates and cultured with TDM containing different hDPCs-sEV concentrations (0, 50, 100 μg/mL) for 7 days. Total RNA was isolated with RNAiso Plus (TaKaRa Biotechnology, Japan) and reverse transcribed into cDNAs using the RevertAid First Strand cDNA Synthesis Kit (Thermo Fisher Scientific, USA). The qRT-PCR was performed on the QuantStudio 6 Flex system (Applied Biosystems, Foster City, CA, USA) with SYBR Premix Ex Taq (TaKaRa Biotechnology, Japan). The $2^{-\Delta\Delta CT}$ method was used to calculate fold changes in target mRNA, and GAPDH was used as the housekeeping gene. The primer sequences used in this study are listed in **Table 1**.

Western blot analysis

The hDPCs were seeded into six-well plates at a density of 10^5cells per well and cultured

with TDM extracts containing different hDPCs-sEV concentrations (0, 50, 100, 200 μg/ml) for 7 days. Total cellular proteins were extracted using the Total Protein Extraction Kit (KeyGene, China). The proteins were separated on polyacrylamide gels and blotted onto a nitrocellulose membrane. The antibodies used to detect the target protein were: alkaline phosphatase (ALP, 1:500; Abcam, UK); Dentin matrix protein-1(DMP-1,1:1000; Santa Cruz, USA); mouse monoclonal to RUNX-2 (1:1000; Abcam, UK); dentin sialophosphoprotein (DSPP, 1:1000; Zen, CN); Rabbit polyclonal to Osteopontin (OPN, 1:1000; Abcam, UK); Mouse monoclonal to Actin (Actin, 1:500; Abcam, UK). After incubation with the second antibody coupled with the species matched HRP (Zen Bioscience, China), the protein bands were visualized with ECL reagent (GE Healthcare Life Sciences, USA). Band intensity was quantified using NIH Image J software[21].

Mini-pig pulp repair model in vivo

All animal experiments were approved by the Animal Experimental Ethics Committee of Sichuan University. Three female miniature pigs (12 months) were purchased from Chengdu Dashuo Bio-Technique Co. Ltd. (Chengdu, China). The teeth of each pig were divided into four groups (n=3 teeth per group), and different materials were used in per group. Grouping is summarized in **Table 2**. The DPCs-sEV concentration in the sEV-TDM group and the DPCs-sEV group was 1 mg/μl.

After anesthetization, using ultra-high-speed dental handpiece (Dentsply Sirona, USA) under deionized water as the coolant, class V or I cavities of 2 mm diameter were prepared on the lingual/occlusal surfaces of experimental teeth and the pulp tissue was mechanically exposed. The experimental materials were placed on the perforation sites immediately after hemostasis and then the cavities were filled with glass ionomer cement (Fuji, Japan). The samples were collected after six weeks, fixed with 4% paraformaldehyde and then scanned with micro-computed tomography (Siemens, Germany). The tissue specimens were demineralized in 10% EDTA for 3 months, sliced into 5 mm thick sections following dehydration and embedded in paraffin for H&E stain as well as Masson's trichrome staining (Baso Diagnostic Inc., China).

Statistical analysis

All *in vitro* experiments were performed in triplicates and repeated at least 3 times. Data

were analyzed using GraphPad Prism v8.0 (GraphPad Software Inc, San Diego, CA, USA) and presented as mean ± standard deviation (SD). Differences between groups were determined using one-way ANOVA. P-value <0.05 was considered statistically significant.

RESULTS

Preparation and characterization of TDM

After mechanical preparation and demineralization, TDM was grounded into fine powder (**Fig. 1**A). SEM micrographs showed that dentinal tubule orifices were visible on the surface of TDM, while TDMP showed micron-sized particles without any dentinal tubule structure (**Fig. 2**B). The protein concentration of the pTDM extracts was 1.71±0.31 μg/μl while that of the hTDM extracts was 1.85±0.23 μg/μl (**Fig.1**C).

Isolation, identification, and characterization of DPCs

The DPCs exhibited typical spindle-shaped morphologic characteristics of mesenchymal cells, and were stained positive for vimentin, a mesenchymal stem cell marker (**Fig. 2**A and **Fig. S1**A-D). The differentiation potential of the hDPCs was confirmed by adipogenic, osteogenic, and neurogenic induction with Oil red staining, Alizarin red staining, and immunofluorescence staining of Nestin, respectively (**Fig. S1**E -H). Flow cytometry analysis showed that hDPCs were positively stained for mesenchymal stem cell markers CD29, CD90, CD44, CD146, CD166, and negatively stained for hematopoietic cell markers CD33, CD34, CD45 as shown in **Fig. S1**I.

Isolation and Identification of sEV

The sEV isolated from DPCs were observed as round and double-membrane structures in TEM. The size of hDPCs-sEV and pDPCs-sEV ranged from 50 to 150 nm in diameter and separately exhibited peaks at 116 nm and 98 nm (**Fig. 2**B). Western blot analysis revealed the presence of CD63, HSP70, and Alix protein markers in the sEV (**Fig. 2**C). In endocytosis experiments, the DiO labeled (green) sEV were found to surround the nuclei after internalization by DPCs (**Fig. 2**D).

Effect of sEV-TDM on cell proliferation and migration

The hDPCs migrated through the polycarbonate membrane as shown in **Fig. 3**A. The TDM extracts and sEV promoted the migration of DPCs compared with the control group (0

μg/ml). In the sEV group, there was a gradual increase in cell migration ability that coincided with an increase in sEV concentration. However, in the sEV-TDM group, the cell migration ability was barely influenced by sEV concentration change (10μg/ml-200μg/ml).

The hDPCs proliferative results are presented in **Fig. 3**B. Under the sEV induced environment, the proliferative ability was elevated when compared to the control group (0μg/ml). Furthermore, the high concentration of sEV (>100μg/ml) did not exhibit any additional effects on the proliferative capacity. TDM extracts combined with sEV induction showed minimal effect on cell proliferation. Meanwhile, at the constant of the same sEV concentration, from day 4, no significant cell proliferation was observed in the TDM extracts groups.

Effect of sEV-TDM on the odontogenic differentiation of hDPCs

The effects of sEV and sEV-TDM on RNA expression levels in odontogenic differentiation of hDPCs are presented in **Fig. 3**C. The sEV-TDM (50 μg/ml+TDM, 100 μg/ml+TDM) induction enhanced the expression of OPN in hDPCs when compared to the control (0μg/ml). Alterations in RUNX2, DSPP, COL-□, and ALP levels in the sEV-TDM group were not significant ($p>0.05$). The TDM extracts (0μg/ml+TDM) significantly up-regulated the hDPC expression levels of DMP-1 ($p<0.001$) and OPN ($p<0.01$) expression of hDPCs when compared with the control. In the sEV group, DMP-1 expression was evidently up-regulated while ALP gene expression was significantly down-regulated at the concentration of 100μg/ml ($P<0.001$) , meanwhile RUNX2 expression was elevated at 50μg/ml ($p<0.05$).

The expression levels of odontoblast-associated proteins after sEV-TDM are shown in **Fig. 3**D. It was revealed that sEV (50μg/ml, 100μg/ml) enhanced the expressions of DMP-1，DSPP and RUNX-2 when compared to the control group (0μg/ml). The sEV-TDM moderately down-regulated RUNX2 expression ($p>0.05$) and significantly elevated the expression of DSPP ($p<0.01$) and DMP-1 ($p<0.01$) in hDPCs.

The pulp capping material of sEV-TDM in miniature pigs

The mini-pig dental pulp defect model preparation procedures are presented in **Fig. S**2A-D. The models with pulp capping and glass-ionomer cement sealed were intact after six weeks of pulp capping. There was a high-density shade at perforation in the TDM, sEV-TDM,

and MTA groups. The incomplete mineralization image was shown in the sEV group (**Fig. S2**E and **Fig. 4**a-d).

The thickness of the regenerated mineralized tissue in the TDM, sEV-TDM, MTA, and sEV groups are shown in **Table 3**. The dentin mineralized layers of the MTA group were thicker than those of the TDM and the sEV-TDM groups. There were no statistically significant differences in the hard tissue bridge max thickness was detected among the TDM, the sEV-TDM, and the MTA groups ($p>0.05$). However, an incomplete mineralized tissue was observed in 4 samples of the sEV group which failed to seal the perforation. There was no obvious mineralized tissue was found in the other 5 samples of the sEV group.

Histological analyses revealed a complete regeneration of the dentin bridge and tertiary dentin matrix in the TDM, sEV-TDM, and MTA groups, but not in the sEV group (**Fig. 4**e-t). In the dental pulp tissue next to the dentin bridge, polarizing and tall columnar odontoblast-like cells were observed in the TDM and the sEV-TDM groups (**Fig. 4**A and B). The reparative dentin of the MTA group appeared close to the osteoid dentin, and the cells were cubic or short column-shaped (**Fig. 4**D). In the sEV group, the reparative dentin layer was incomplete with calcified masses. Moreover, inflammatory reaction in the form of proliferation of fibrous tissue was observed in the pulp tissue (**Fig. 4**C).

DISCUSSION

The generation of high-quality reparative dentin is a critical factor for successful Vital Pulp therapy after externally stimulated pulp injury[22]. This process involves the recruitment and differentiation of odontoblast-like cells and the synthesis of new dentine-like hard tissues. To improve the properties of pulp capping materials for better biological functions, and to promote the balance between inflammation and regeneration, it is necessary to understand the biological regeneration mechanism of the dental pulp-dentin complex[23]. Studies have documented that the formation of reactionary dentin is correlated to the release of bioactive molecules from the demineralized dentin matrix, and a series of DPC associated autocrine and paracrine signaling mediators[5, 22]. Extracellular vesicles (EVs), are important cell secretion components used to promote tissue regeneration[13, 14]. Therefore, in this study, TDM combined with sEV was found to exhibit superior effects in promoting the regeneration of reparative

dentin.

Prior studies have reported that EVs influence the proliferation, invasion, and migration abilities of the recipient cells[15]. Chen et al.[9] documented that DPCs cultured in high TDMP extract concentrations showed decreased cell line proliferative ability. The proliferative ability was, however, elevated at low concentrations. This study revealed that the sEV promoted cell proliferation, while the sEV-TDM inhibited cell proliferation. This is attributed to the fact that the cell proliferation and differentiation processes are inconsistent with different regulatory mechanisms and complex influencing factors. The transwell assay also showed that sEV and sEV-TDM promoted DPCs migration. However, the change in sEV concentration did not alter the migratory capacity of the cells in the sEV-TDM groups. The TDM extracts effectively promoted cell migration, masking the role of sEV.

The TDM powder releases an extensive amount of soluble dentin matrix proteins in a liquid environment[8]. The TDM extracts has been shown to promote mesenchymal stem cell differentiation into odontogenic cell lineages[6, 7, 9]. The EVs isolated from differentiating DPSCs cultured in odontogenic differentiation media can also induce the odontogenic differentiation of cells[15, 17]. We found that there were notable differences in the effect of sEV-TDM and sEV on inducing lineage-specific differentiation of DPCs. There was a significant up-regulation of DSPP, DMP-1, RUNX-2, OPN in sEV cultured groups, however, sEV down-regulated alkaline phosphatase (ALP). Under sEV-TDM culture conditions, ALP and OPN were up-regulated while DMP-1 and RUNX-2 were down-regulated in DPCs (**Fig. 3**C). ALP promotes calcification and the expression level of ALP is positively correlated with the degree of calcification[24]. DSPP, DMP-1, and OPN are members of the SIBLING-family that are secreted into the extracellular matrix during tooth and bone formation as well as mineralization[25, 26]. RUNX-2 is a transcription factor that regulates the osteogenic differentiation of cells and is involved in bone and teeth formation and development[27]. The DMP-1 and DSPP protein expression levels were elevated in the sEV and sEV-TDM groups when compared to the control group, while sEV-TDM did not exhibit any significant effect in promoting the expression levels of ALP and OPN for 7 days of induction in hDPCs (**Fig. 3**D).

The mini-pig model of dental pulp defect is considered a classic model for evaluating pulp injury and repair[28]. Studies have established that the exposed human dental pulp covered

with MTA and BIODENTINE can form a mineralized seal in 6-8 weeks[29, 30]. TDM and sEV-TDM induced calcified hard tissue barrier and reactionary dentin were similar. The effect of the pulp-capping material was evaluated using radiographs, micro-CT, and histological analysis. Pulp capping with TDM and sEV-TDM resulted in complete dentin bridge regeneration, without tunnel defect (**Fig. 4**A and B).

In the sEV group, it was difficult to seal the exposed pulp at the beginning of capping because sEV solution was incapable of residing in situ, hence there was no complete mineralized structure (**Fig. 4**C). The sEV concentration used in the experimental group was 1 mg/μl. Studies have reported that the concentration can influence the effect of sEV on the differentiation of angioblasts and endothelial cells. In addition, some studies have also revealed that the effect of low EVs concentration are better when compared to high concentrations[31-33]. In the mineralized layer near the pulp, short column or flat fibroblast-like cells were observed in the MTA group, while columnar cell layers were observed in the TDM and sEV-TDM groups (**Fig. 4**D). Till et al.[4] reported cells similar to fibroblasts but not odontoblast-like cells after pulp capping of human third molars with MTA. The visible cells in the cell layer of the mineralized tissue appeared cuboidal or flat, with some cell processes projecting towards the mineralized tissue[34, 35].

In vivo experiments confirmed that the dentin mineralized layers of sEV-TDM were thicker compared to those in the TDM group. *In vitro*, DPCs-sEV improved the dentin induction ability of dental pulp stem cells. As a mineralized extracellular matrix component, TDM is considered a natural scaffold material with diverse non-mineralized dentin matrix components such as glycosaminoglycan, chondroitin sulfate, type I collagen, BMP, and DSP, among others[8]. EVs can bind to type □ collagen and fibronectin in a dose-dependent and saturable manner[15]. Therefore, the sEV and dentin matrix proteins loaded in TDM can be released into the dental pulp tissue and endocytosed by cells in the dental pulp to promote mineralization.

CONCLUSION

In summary, this study showed that sEV-TDM effectively recruits DPCs, induces the odontogenic process, and stimulates the formation of reactive dentin. Its composition of

sEV-TDM has more suitable odontogenic inductivity when compared to MTA. Therefore, sEV-TDM is recommended as a potential bioactive pulp capping material for vital pulp therapy.

References

1. Dammaschke T, Steven D, Kaup M, Ott KH. Long-term survival of root-canal-treated teeth: a retrospective study over 10 years. J Endod 2003;29:638-43.

2. Smaïl-Faugeron V, Glenny AM, Courson F, Durieux P, Muller-Bolla M, Fron Chabouis H. Pulp treatment for extensive decay in primary teeth. Cochrane Database Syst Rev 2018;5:CD003220.

3. Prati C, Gandolfi MG. Calcium silicate bioactive cements: Biological perspectives and clinical applications. Dent Mater 31:351-70.

4. Dammaschke T, Nowicka A, Lipski M, Ricucci D. Histological evaluation of hard tissue formation after direct pulp capping with a fast-setting mineral trioxide aggregate (RetroMTA) in humans. Clin Oral Investig 2019.

5. Murray PE, About I, Lumley PJ, Smith G, Franquin JC, Smith AJ. Postoperative pulpal and repair responses. J Am Dent Assoc 2000;131:321-9.

6. Li R, Guo W, Yang B, et al. Human treated dentin matrix as a natural scaffold for complete human dentin tissue regeneration. Biomaterials 2011;32:4525-38.

7. Yang B, Chen G, Li J, et al. Tooth root regeneration using dental follicle cell sheets in combination with a dentin matrix - based scaffold. Biomaterials 2012;33:2449-61.

8. Li J, Yang H, Lu Q, et al. Proteomics and N-glycoproteomics analysis of an extracellular matrix-based scaffold-human treated dentin matrix. J Tissue Eng Regen Med 2019;13:1164-77.

9. Chen J, Cui C, Qiao X, et al. Treated dentin matrix paste as a novel pulp capping agent for dentin regeneration. J Tissue Eng Regen Med 2017;11:3428-36.

10. Farges JC, Alliot-Licht B, Renard E, et al. Dental Pulp Defence and Repair Mechanisms in Dental Caries. Mediators Inflamm 2015;2015:230251.

11. Xuan K, Li B, Guo H, et al. Deciduous autologous tooth stem cells regenerate dental pulp after implantation into injured teeth. Sci Transl Med 2018;10.

12. Liang X, Ding Y, Zhang Y, Tse HF, Lian Q. Paracrine mechanisms of mesenchymal stem cell-based therapy: current status and perspectives. Cell Transplant 2014;23:1045-59.

13. Kalluri R, LeBleu VS. The biology, function, and biomedical applications of exosomes. Science 2020;367.

14. Kourembanas S. Exosomes: vehicles of intercellular signaling, biomarkers, and vectors of cell therapy. Annu Rev Physiol 2015;77:13-27.

15. Huang CC, Narayanan R, Alapati S, Ravindran S. Exosomes as biomimetic tools for stem cell differentiation: Applications in dental pulp tissue regeneration. Biomaterials 2016;111:103-15.

16. Wang HS, Yang FH, Wang YJ, Pei F, Chen Z, Zhang L. Odontoblastic Exosomes Attenuate Apoptosis in Neighboring Cells. J Dent Res 2019;98:1271-8.

17. Hu X, Zhong Y, Kong Y, Chen Y, Feng J, Zheng J. Lineage-specific exosomes promote the odontogenic differentiation of human dental pulp stem cells (DPSCs) through TGFβ1/smads signaling pathway via transfer of microRNAs. Stem Cell Res Ther 2019;10:170.

18. Gronthos S, Brahim J, Li W, et al. Stem cell properties of human dental pulp stem cells. J Dent Res 2002;81:531-5.

19. Zhang Y, Yu M, Dai M, et al. miR-450a-5p within rat adipose tissue exosome-like vesicles promotes adipogenic differentiation by targeting WISP2. J Cell Sci 2017;130:1158-68.

20. Exosomes from differentiating human skeletal muscle cells trigger myogenesis of stem cells and provide biochemical cues for skeletal muscle regeneration. J Control Release 222:107-15.

21. Jensen EC. Quantitative analysis of histological staining and fluorescence using ImageJ. Anat Rec (Hoboken) 2013;296:378-81.

22. da Rosa W, Piva E, da Silva AF. Disclosing the physiology of pulp tissue for vital pulp therapy. Int Endod J 2018;51:829-46.

23. Giraud T, Jeanneau C, Rombouts C, Bakhtiar H, Laurent P, About I. Pulp capping materials modulate the balance between inflammation and regeneration. Dent Mater 2019;35:24-35.

24. Groeneveld MC, Everts V, Beertsen W. Alkaline phosphatase activity in the periodontal ligament and gingiva of the rat molar: its relation to cementum formation. J Dent Res 1995;74:1374-81.

25. Butler WT, Ritchie H. The nature and functional significance of dentin extracellular matrix proteins. Int J Dev Biol 1995;39:169-79.

26. Staines KA, MacRae VE, Farquharson C. The importance of the SIBLING family of proteins on skeletal mineralisation and bone remodelling. J Endocrinol 2012;214:241-55.

27. Vimalraj S, Arumugam B, Miranda PJ, Selvamurugan N. Runx2: Structure, function, and phosphorylation in osteoblast differentiation. Int J Biol Macromol 2015;78:202-8.

28. Nakashima M, Iohara K, Bottino MC, Fouad AF, Nör JE, Huang GT. Animal Models for Stem Cell-Based Pulp Regeneration: Foundation for Human Clinical Applications.

Tissue Eng Part B Rev 2019;25:100-13.

29. Aeinehchi M, Eslami B, Ghanbariha M, Saffar AS. Mineral trioxide aggregate (MTA) and calcium hydroxide as pulp-capping agents in human teeth: a preliminary report. Int Endod J 2003;36:225-31.

30. Koubi G, Colon P, Franquin JC, et al. Clinical evaluation of the performance and safety of a new dentine substitute, Biodentine, in the restoration of posterior teeth - a prospective study. Clin Oral Investig 2013;17:243-9.

31. Anderson JD, Johansson HJ, Graham CS, et al. Comprehensive Proteomic Analysis of Mesenchymal Stem Cell Exosomes Reveals Modulation of Angiogenesis via Nuclear Factor-KappaB Signaling. Stem Cells 2016;34:601-13.

32. McBride JD, Rodriguez-Menocal L, Guzman W, Candanedo A, Garcia-Contreras M, Badiavas EV. Bone Marrow Mesenchymal Stem Cell-Derived CD63+ Exosomes Transport Wnt3a Exteriorly and Enhance Dermal Fibroblast Proliferation, Migration, and Angiogenesis In Vitro. Stem Cells Dev 2017;26:1384-98.

33. Liang X, Zhang L, Wang S, Han Q, Zhao RC. Exosomes secreted by mesenchymal stem cells promote endothelial cell angiogenesis by transferring miR-125a. J Cell Sci 2016;129:2182-9.

34. Bakhtiar H, Aminishakib P, Ellini MR, et al. Dental Pulp Response to RetroMTA after Partial Pulpotomy in Permanent Human Teeth. J Endod 2018;44:1692-6.

35. Oliveira TM, Moretti AB, Sakai VT, et al. Clinical, radiographic and histologic analysis of the effects of pulp capping materials used in pulpotomies of human primary teeth. Eur Arch Paediatr Dent 2013;14:65-71.

FIGURE LEGENDS

FIGURE 1-The preparation of TDM. (A) TDM was fabricated from the isolated tooth and used to prepare aqueous TDM extracts after triturated. (B) SEM observation of surface morphology of TDM and TDMP. (C) The protein concentration of pTDM extraction and hTDM extraction.

FIFURE 2-Isolation and identification of DPCs and sEV. (A) Culture and identification of DPCs. The DPCs were the typical morphologic characteristics of mesenchymal cells in fibroblastic and spindle-shaped (a, b) and were positive for vimentin (c) and negative for CK-14 (d). (B) The sEV identification of TEM (a, c) and the size distribution of sEV with NTA (b, d). (C) The expression of labeled proteins in sEV was detected by western blot of CD63, HSP70, Alix. (D) Endocytosis of sEV by DPCs. The cell nucleus is visualized with the nuclear marker DAPI (blue, a, e). The cytoskeleton was visualized with the Phalloidin (red, b, f). The sEV is visualized with DiO (green, c, g).

FIGURE 3-The effect of sEV-TDM on hDPCs in vitro. (A) The DPCs migrated through the polycarbonate membrane of the transwell chamber in the sEV group and the sEV-TDM attraction group with different concentrations of sEV. (B) The proliferation of DPCs after treatment with sEV in the α-MEM group and TDM attraction group. (C) The mRNA levels of odontogenic differentiation marker genes DSPP, DMP-1, ALP, COL-Ⅰ, OPN, and RUNX-2 after treatment with α-MEM group and TDM attraction group via different concentrations of sEV. (D) The protein DSPP, DMP-1, ALP, OPN, and RUNX-2 expressions of TDM attraction and sEV. * $p < 0.05$, ** $p < 0.01$, and *** $p < 0.001$.

FIGURE 4-The sEV-TDM as pulp capping material, evaluated in vivo in miniature swine. (A) The TDM group. (B) The sEV-TDM group. (C) The sEV group. (D) The MTA group. Micro-CT images (a-d), the HE (e-l), and Masson (m-t) staining after 6 weeks of direct pulp capping showed that complete dentin bridge formation could be seen in TDM group, sEV-TDM group and MTA group, but not in the sEV group. D, dentin; P, pulp tissue; DB, dental bridge.

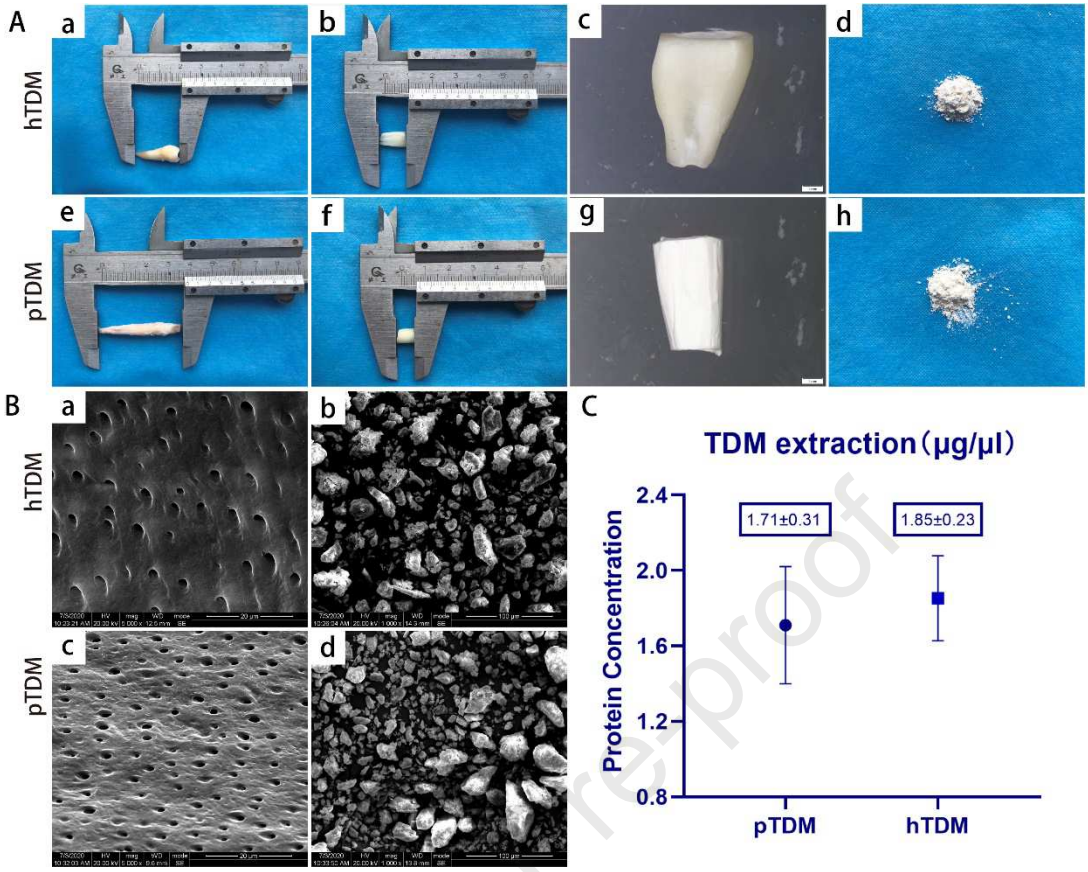

FIGURE 1-The preparation of TDM. (A) TDM was fabricated from the isolated tooth and used to prepare aqueous TDM extracts after triturated. (B) SEM observation of surface morphology of TDM and TDMP. (C) The protein concentration of pTDM extraction and hTDM extraction.

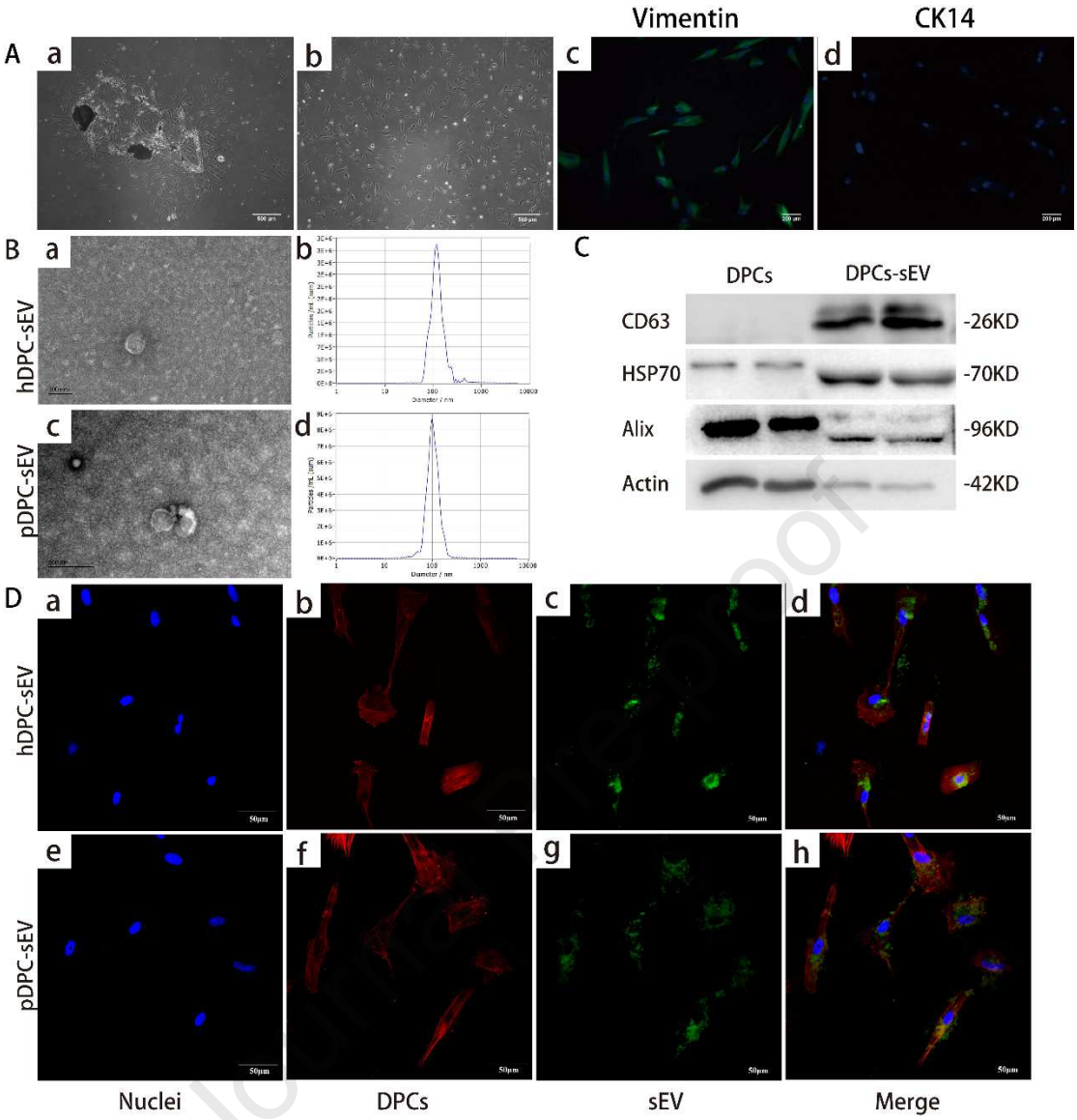

FIFURE 2-Isolation and identification of DPCs and sEV. (A) Culture and identification of DPCs. The DPCs were the typical morphologic characteristics of mesenchymal cells in fibroblastic and spindle-shaped (a, b) and were positive for vimentin (c) and negative for CK-14 (d). (B) The sEV identification of TEM (a, c) and the size distribution of sEV with NTA (b, d). (C) The expression of labeled proteins in sEV was detected by western blot of CD63, HSP70, Alix. (D) Endocytosis of sEV by DPCs. The cell nucleus is visualized with the nuclear marker DAPI (blue, a, e). The cytoskeleton was visualized with the Phalloidin (red, b, f). The sEV is visualized with DiO (green, c, g).

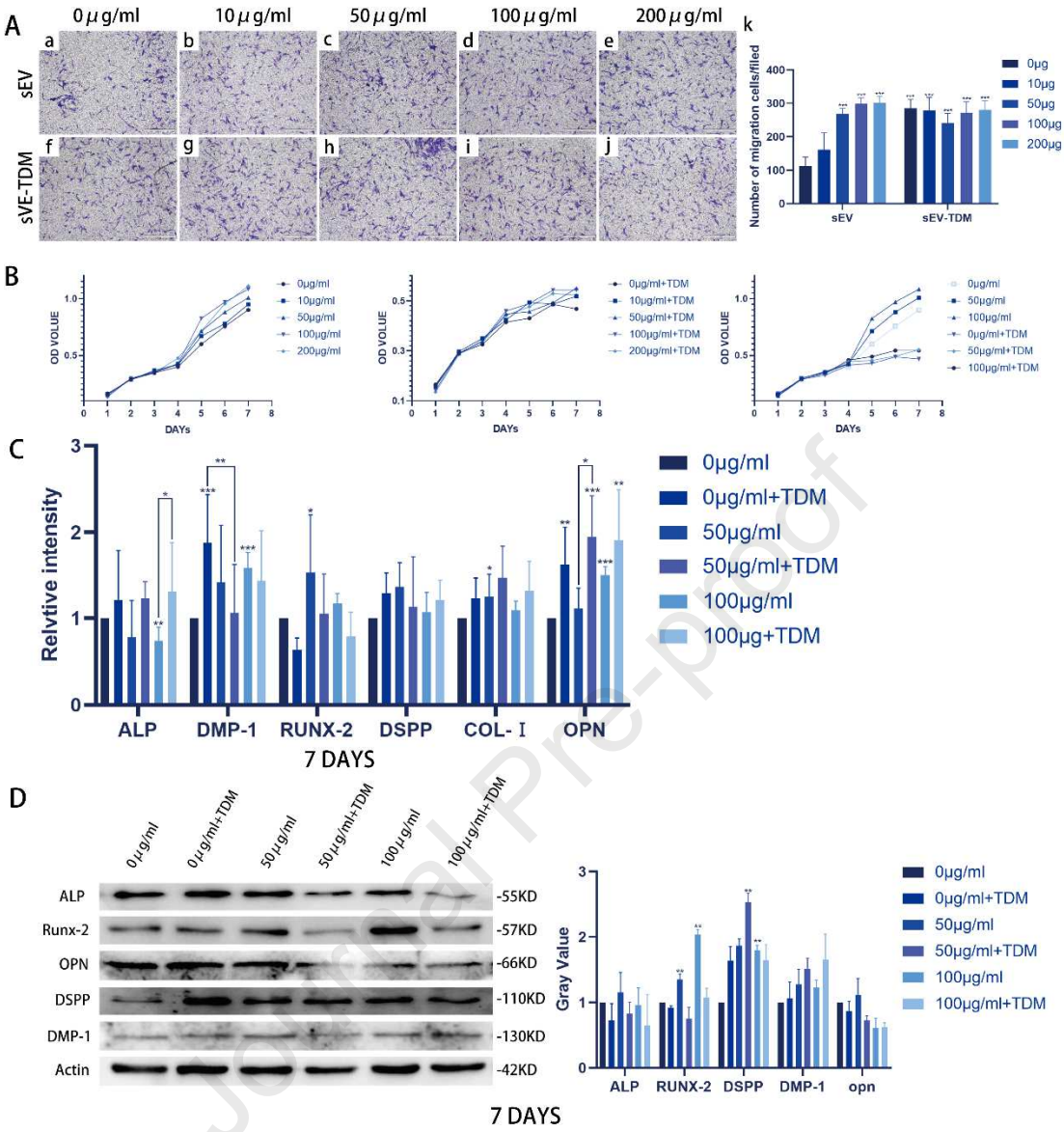

FIGURE 3-The effect of sEV-TDM on hDPCs in vitro. (A) The DPCs migrated through the polycarbonate membrane of the transwell chamber in the sEV group and the sEV-TDM attraction group with different concentrations of sEV. (B) The proliferation of DPCs after treatment with sEV in the α-MEM group and TDM attraction group. (C) The mRNA levels of odontogenic differentiation marker genes DSPP, DMP-1, ALP, COL-□, OPN, and RUNX-2 after treatment with α-MEM group and TDM attraction group via different concentrations of sEV. (D) The protein DSPP, DMP-1, ALP, OPN, and RUNX-2 expressions of TDM attraction and sEV. * $p < 0.05$, ** $p < 0.01$, and *** $p < 0.001$.

1

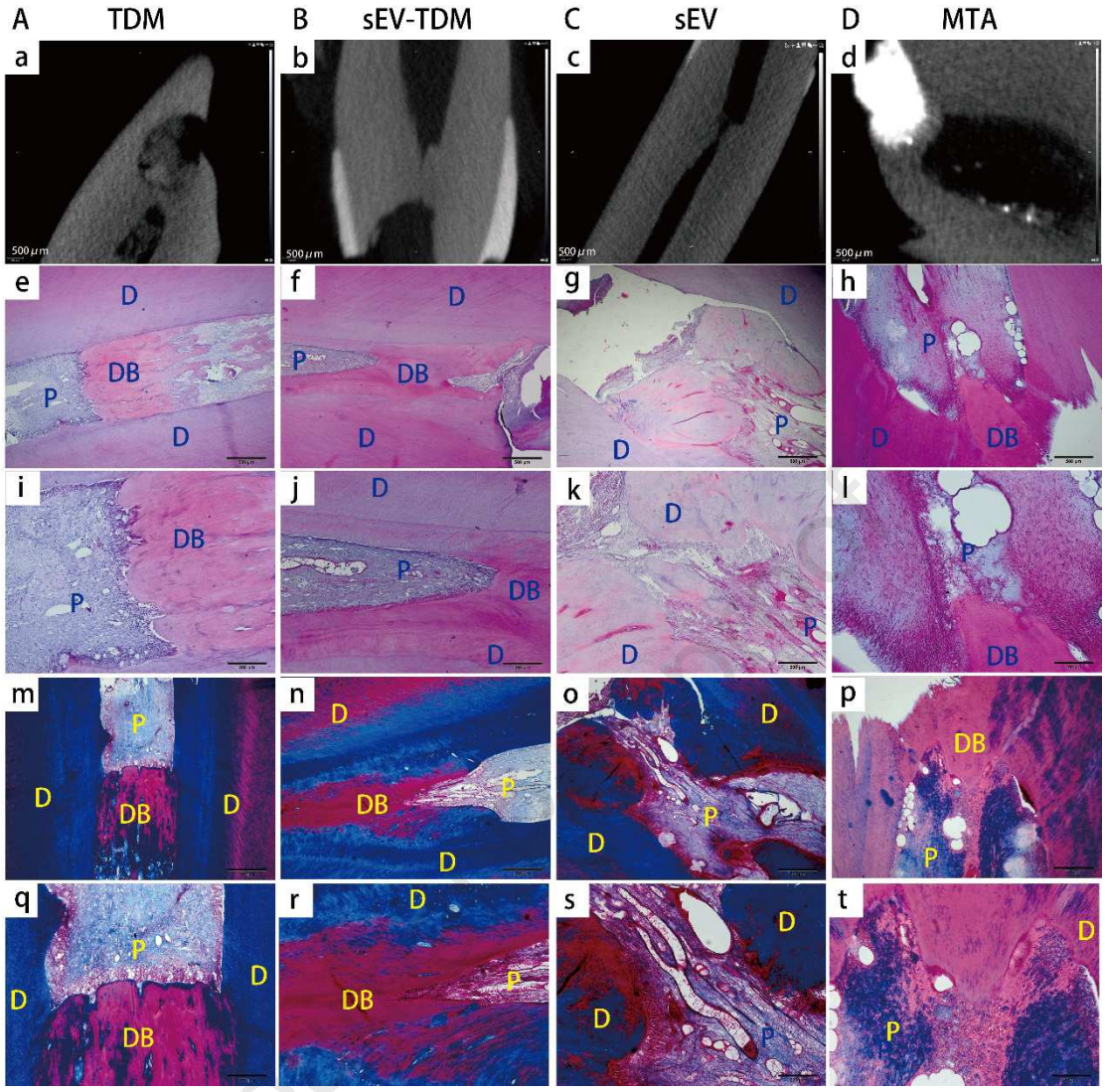

FIGURE 4-The sEV-TDM as pulp capping material, evaluated in vivo in miniature swine. (A) The TDM group. (B) The sEV-TDM group. (C) The sEV group. (D) The MTA group. Micro-CT images (a-d), the HE (e-l), and Masson (m-t) staining after 6 weeks of direct pulp capping showed that complete dentin bridge formation could be seen in TDM group, sEV-TDM group and MTA group, but not in the sEV group. D, dentin; P, pulp tissue; DB, dental bridge.

Table 1. The primer sequences used for RT -qPCR

Gene	Forward sequence/reverse sequence
GAPDH	5`-CTTTGGTATCGTGGAAGGACTC-3`/
	5`-GTAGAGGCAGGGATGATGTTCT-3`
DMP-1	5`-CTCGCACACACTCTCCCACTCAAA-3`/
	5`-TGGCTTTCCTCGCTCTGACTCTCT-3`
ALP	5`-TAAGGACATCGCCTACCAGCTC-3`/
	5`-TCTTCCAGGTGTCAACGAGGT-3`
DSPP	5`-GGAGCCACAAACAGAAGCA-3`/
	5`-TGGACAACAGCGACATCCT-3`
RUNX-2	5`-CTTTACTTACACCCCGCCAGTC-3`/
	AGAGATATGGAGTGCTGCTGGTC-3`
OPN	5`-CAGTTGTCCCCACAGTAGACAC-3`/
	5`-GTGATGGTCCTCGTCTGTAGCATC-3`
COL-Ⅰ	5`-AACATGGAGACTGGTGAGACCT-3`/
	5`-CGCCATACTCGAACTGGAACT-3`

1 **Table 2**. The Animal grouping and model design

Pulp-capping agent	Teeth total Number	The observation time	The surgical site
sEV	9	6 weeks	Left maxillary region
TDM	9	6 weeks	Right maxillary region
sEV-TDM	9	6 weeks	Right mandibular region
MTA	9	6 weeks	Lift mandibular region

2

3

Table 3. The Mean Value and Standard Deviation of the Maximum Thickness of a Hard Tissue Bridge Formed after Capping Treatment with MTA, sEV, sEV-TDM and TDM

Pulp-capping agent	Teeth total Number	Continuity of mineralized tissue			Hard tissue bridge max thickness (μm)
		None	Partial	Complete	
sEV	9	5	4	0	--
TDM	9	1	0	9	84.7±26.5
sEV-TDM	9	0	0	9	97.7±25.6
MTA	9	0	0	9	110.2±21.7

Supplementary Materials

FIGURE S1-The identification, and characterization of DPCs. (A, B, C, and D) The micrographs of cultured DPCs from dental pulp tissue. (E) After adipogenic culture conditions that lipid droplets were shown by Oil red staining. (F) After osteogenic inductive, mineralized nodules can be observed with Alizarin red staining. (G and H) After neurogenic induction, the morphologic of induced hDPCs changed, and the neurogenic maker Nestin can be detected. (I) Flow cytometric analysis showed that hDPCs were stained positively for CD29, CD90, CD44, CD146, CD166, and negatively for CD33, CD34, CD45.

FIGURE S2-Imaging results of sEV-TDM as Pulp capping material in miniature swine. (A, B, and C) The model of dental pulp defect was made on the teeth of miniature swine, (D) X-ray films were taken after pulp capping. (E) Micro-CT scanning (1mm) and X-ray images after 6 weeks of direct pulp capping.

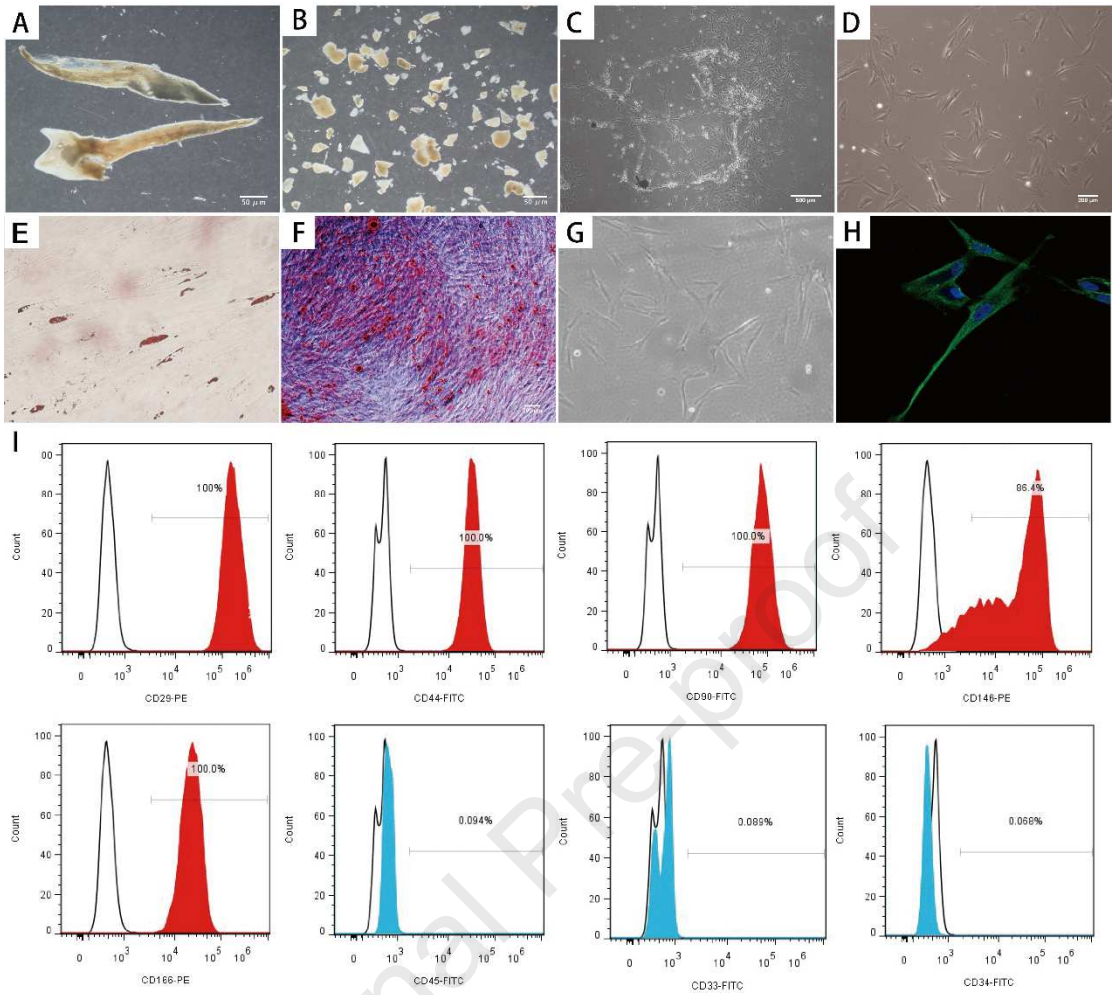

FIGURE S1-The identification, and characterization of DPCs. (A, B, C, and D) The micrographs of cultured DPCs from dental pulp tissue. (E) After adipogenic culture conditions that lipid droplets were shown by Oil red staining. (F) After osteogenic inductive, mineralized nodules can be observed with Alizarin red staining. (G and H) After neurogenic induction, the morphologic of induced hDPCs changed, and the neurogenic maker Nestin can be detected. (I) Flow cytometric analysis showed that hDPCs were stained positively for CD29, CD90, CD44, CD146, CD166, and negatively for CD33, CD34, CD45.

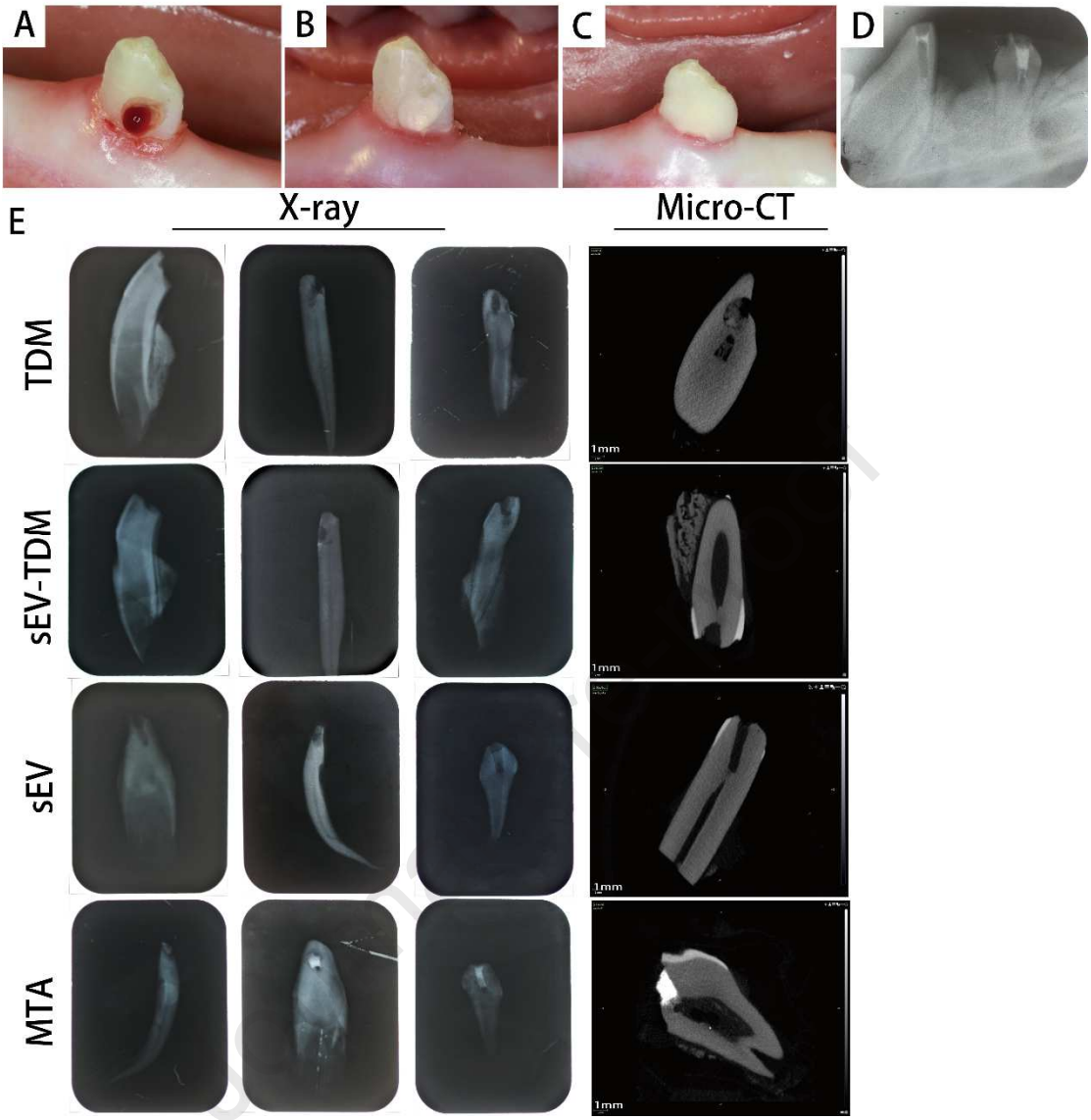

FIGURE S2-Imaging results of sEV-TDM as Pulp capping material in miniature swine. (A, B, and C) The model of dental pulp defect was made on the teeth of miniature swine, (D) X-ray films were taken after pulp capping. (E) Micro-CT scanning (1mm) and X-ray images after 6 weeks of direct pulp capping.

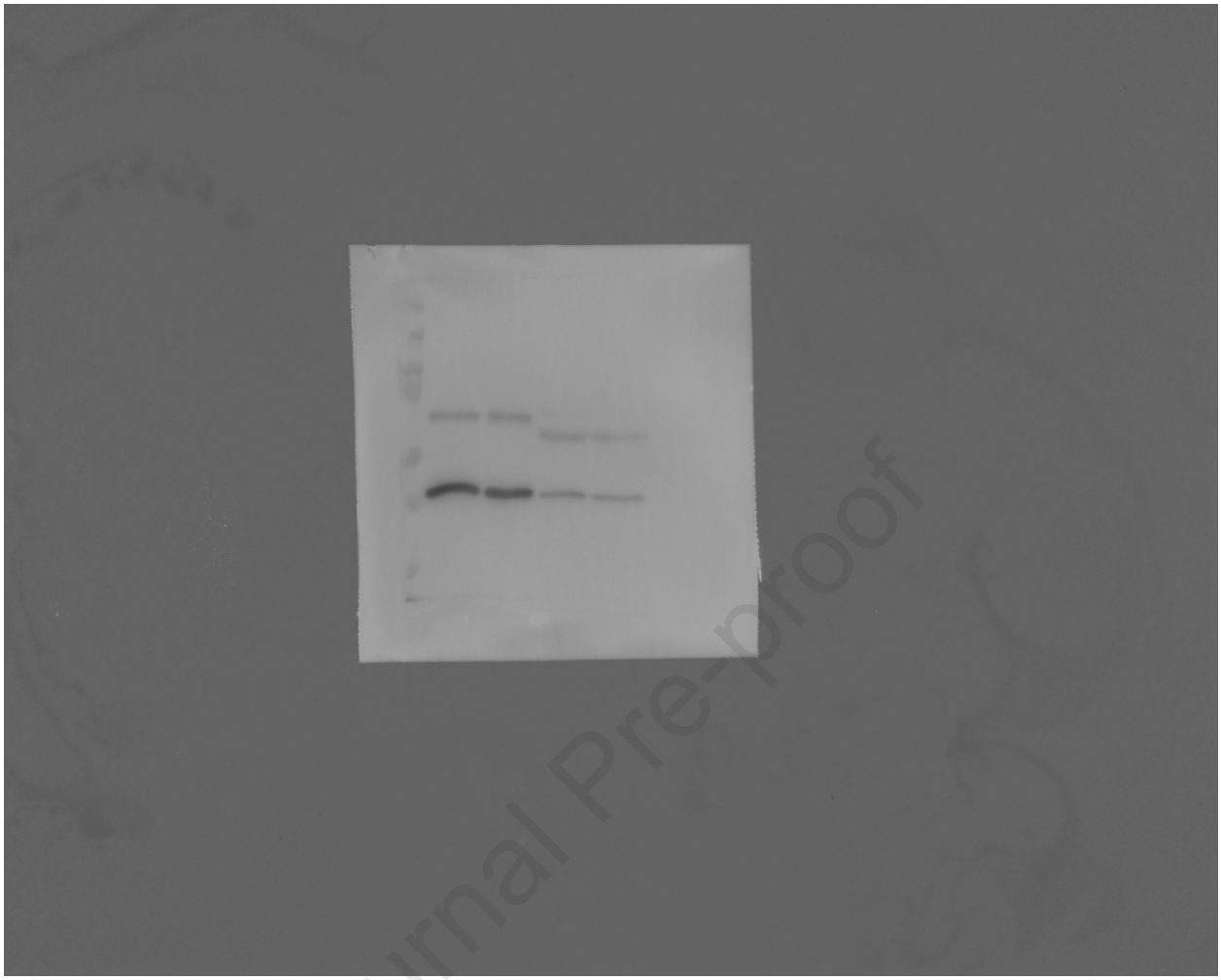

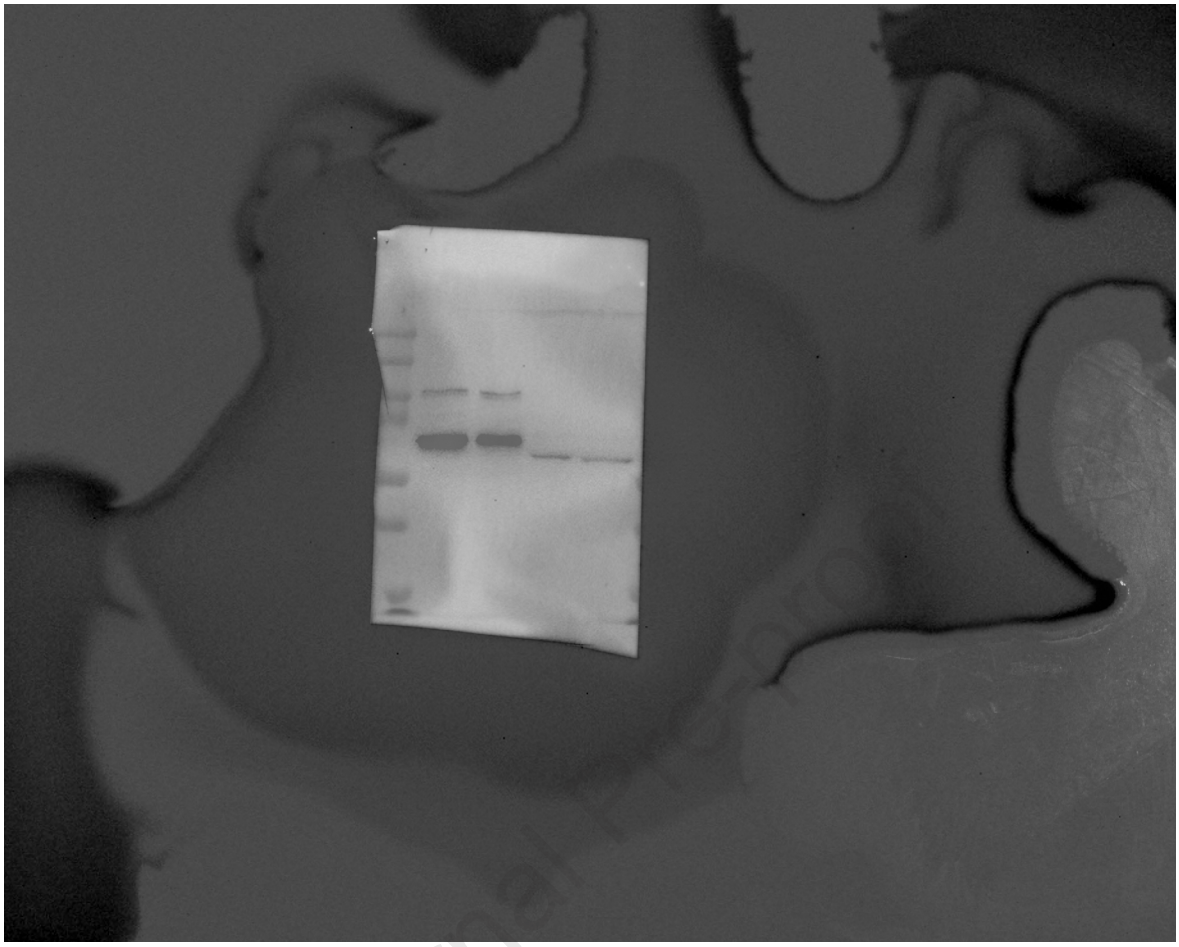

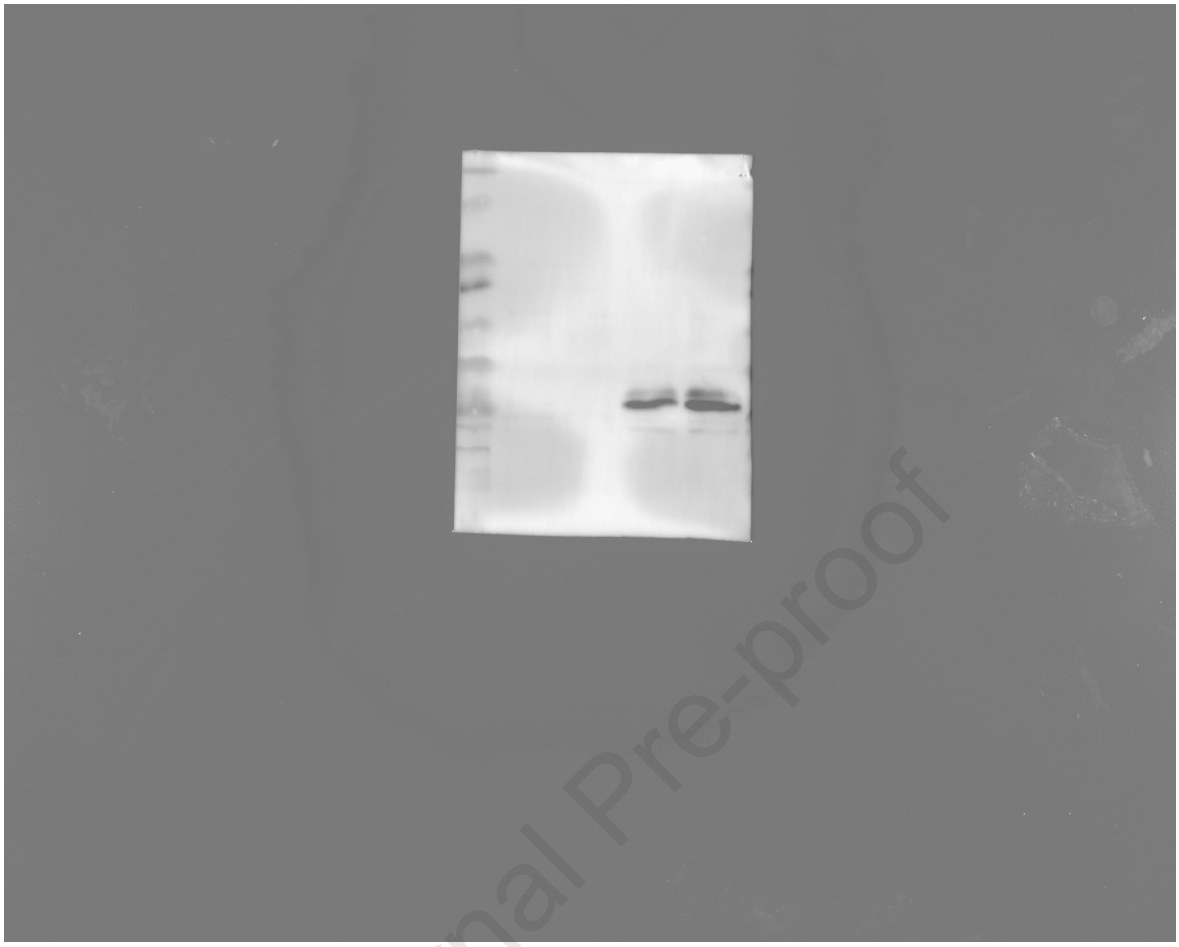

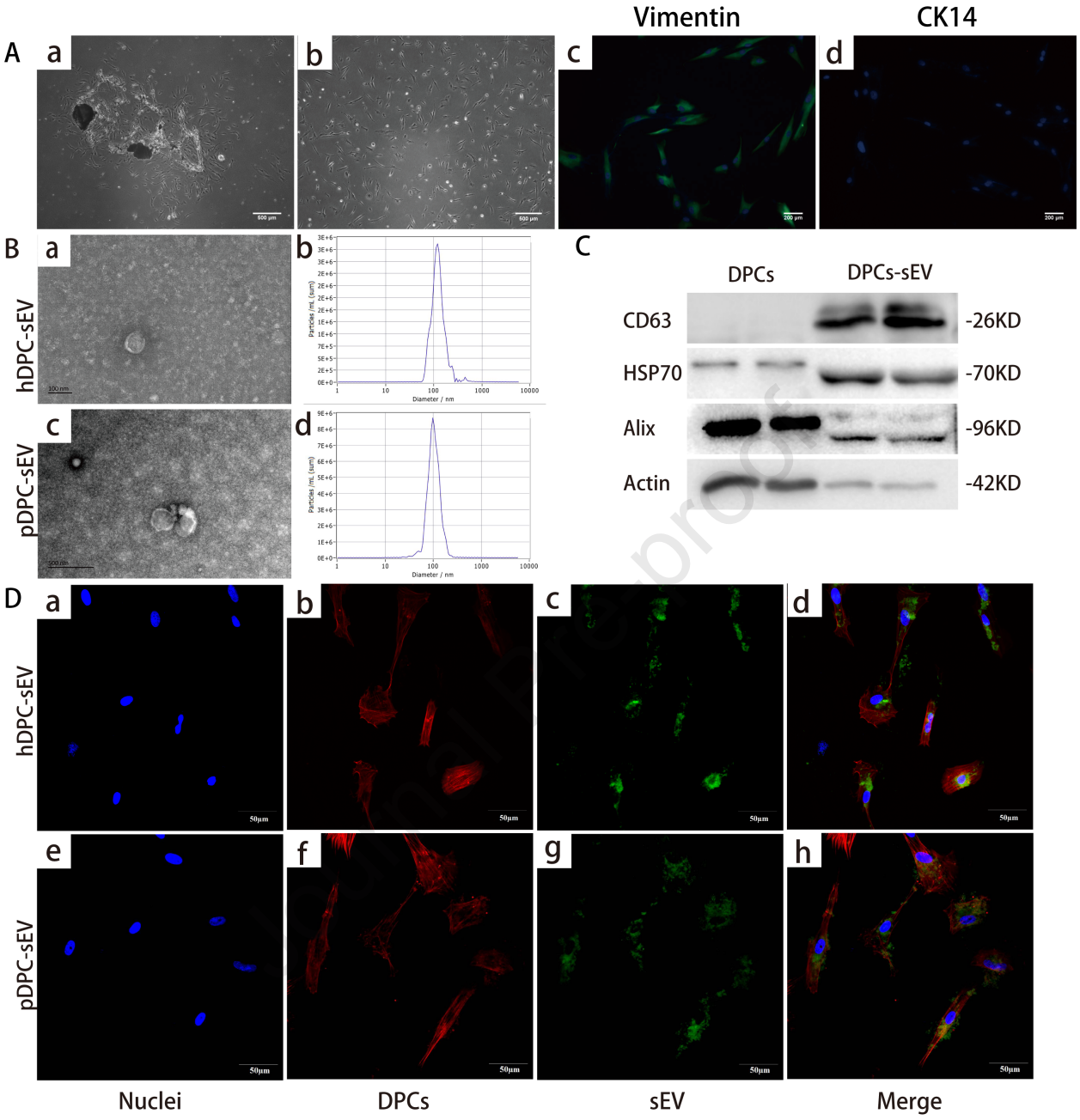
A
a
b
Vimentin
c
CK14
d
B
a
b
hDPC-sEV
c
d
pDPC-sEV
C
DPCs
DPCs-sEV
CD63
-26KD
HSP70
-70KD
Alix
-96KD
Actin
-42KD
D
a
b
c
d
hDPC-sEV
e
f
g
h
pDPC-sEV
Nuclei
DPCs
sEV
Merge

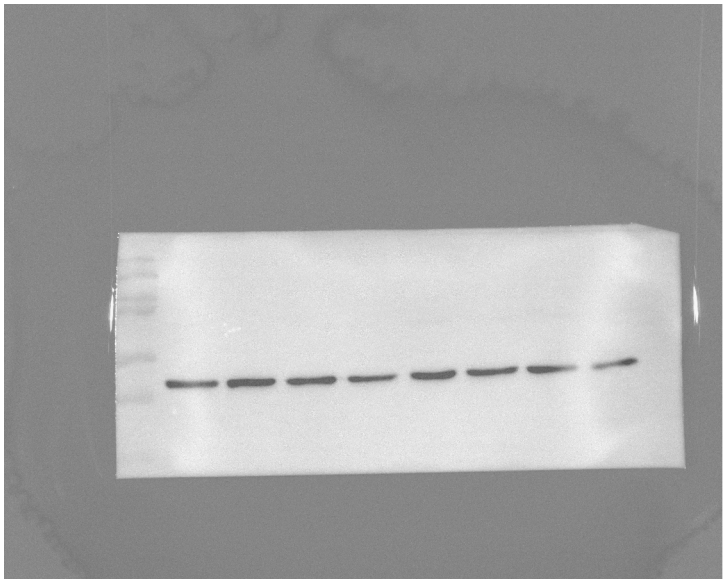

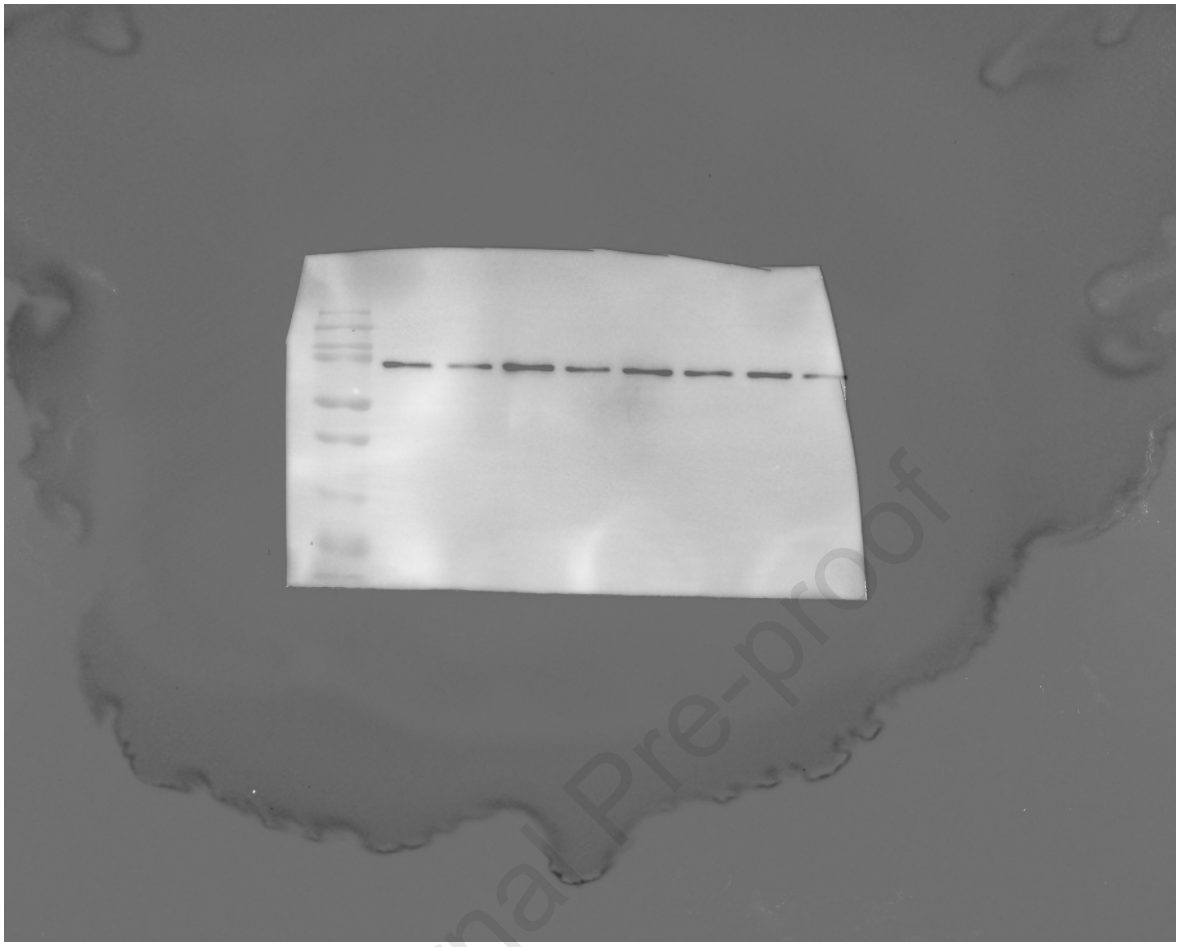

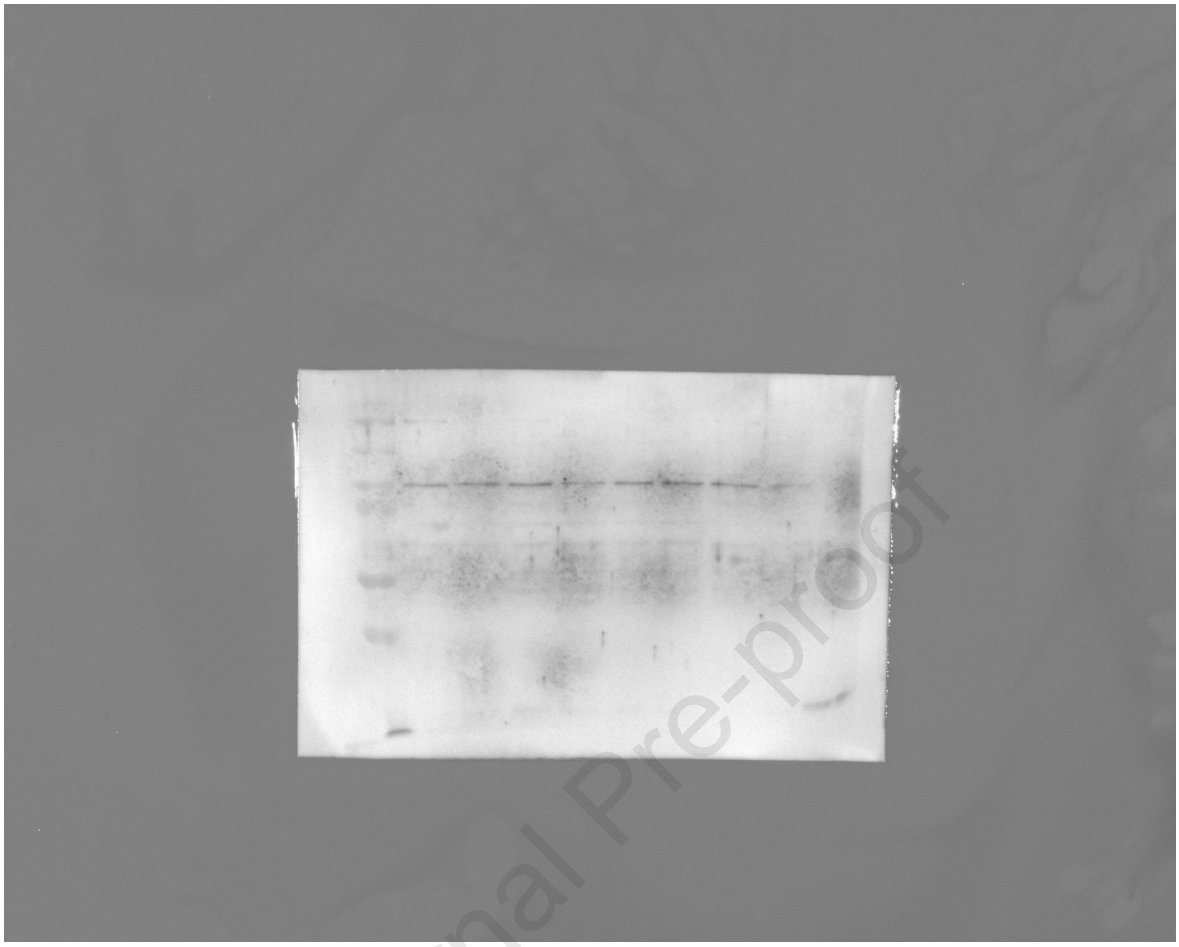

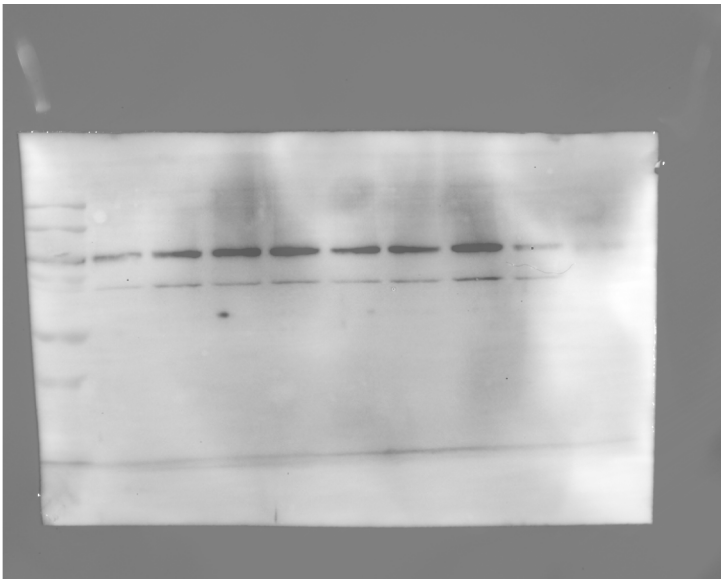

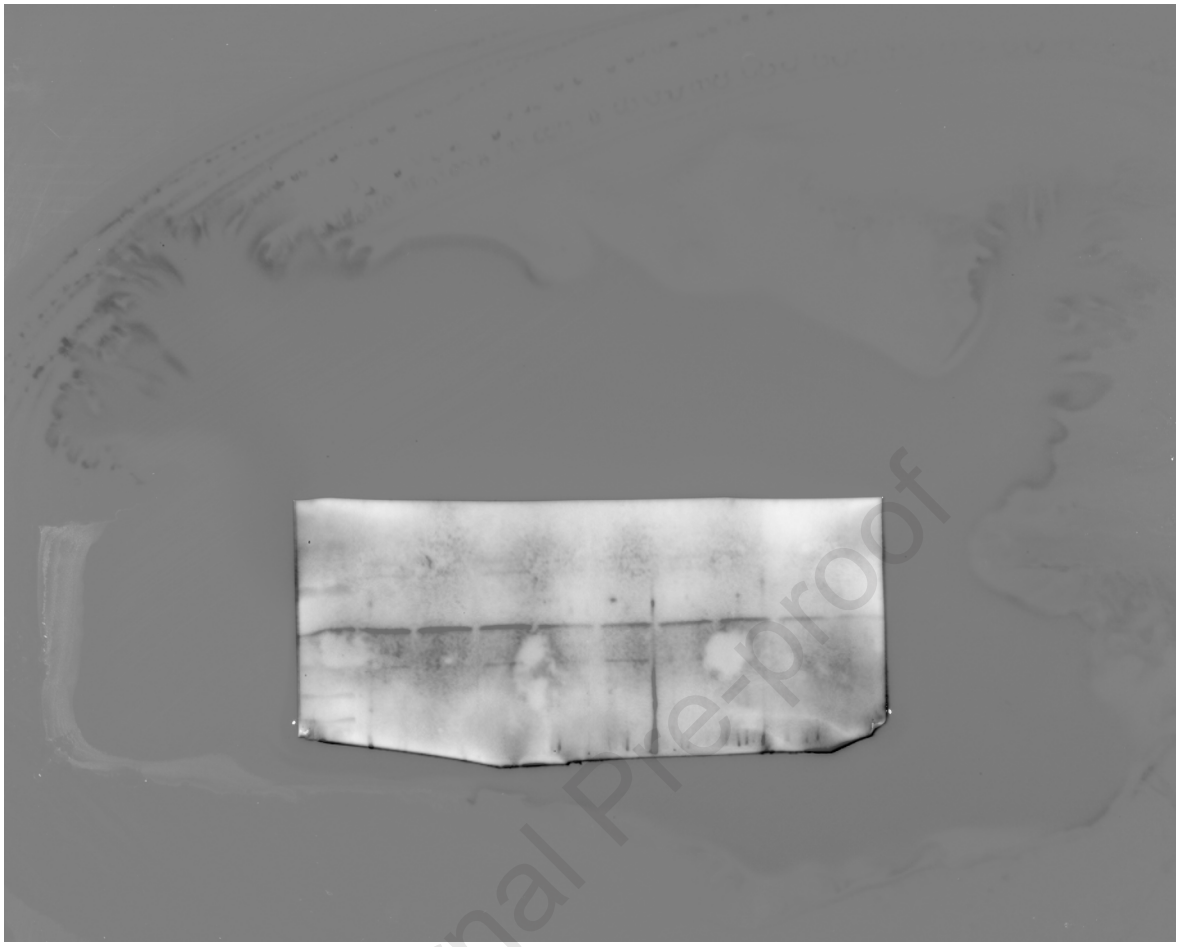

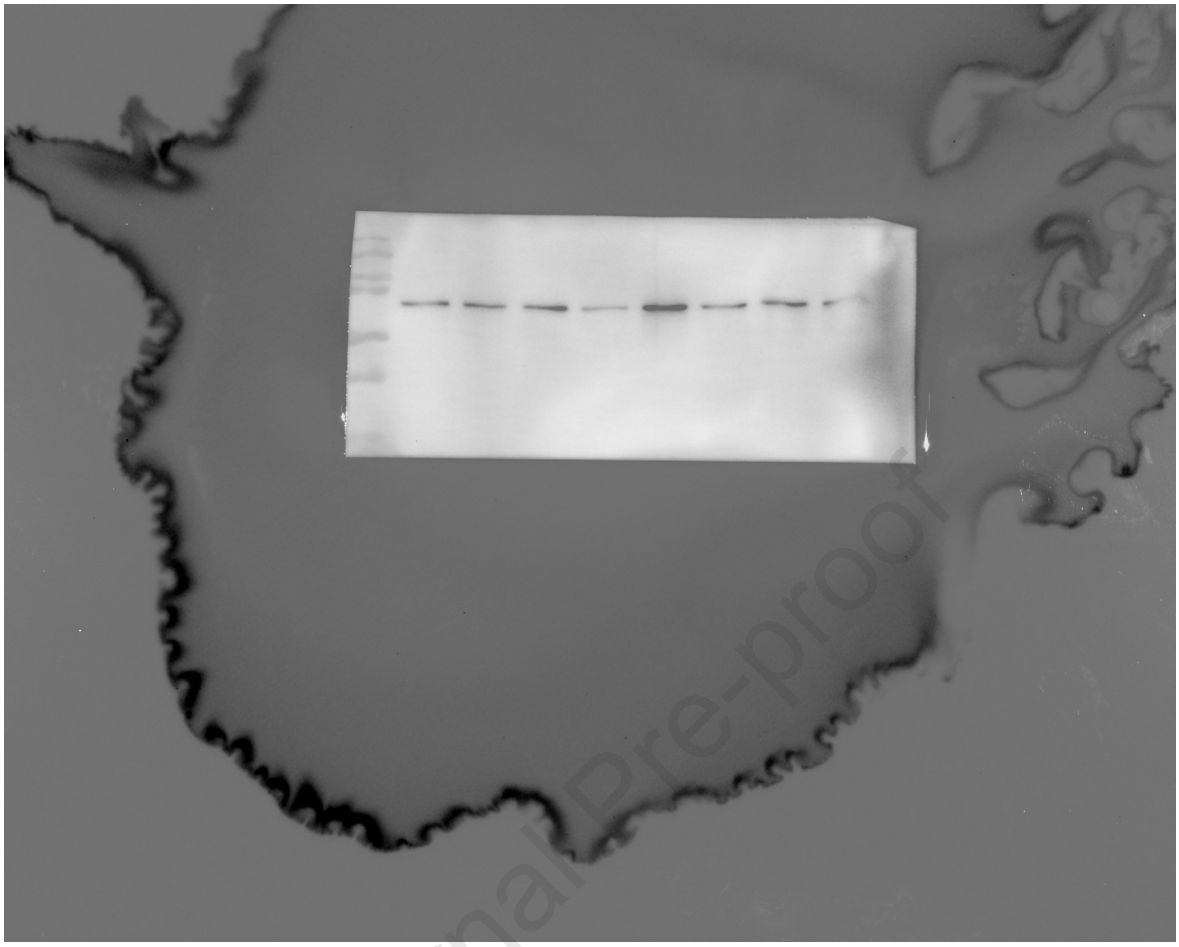

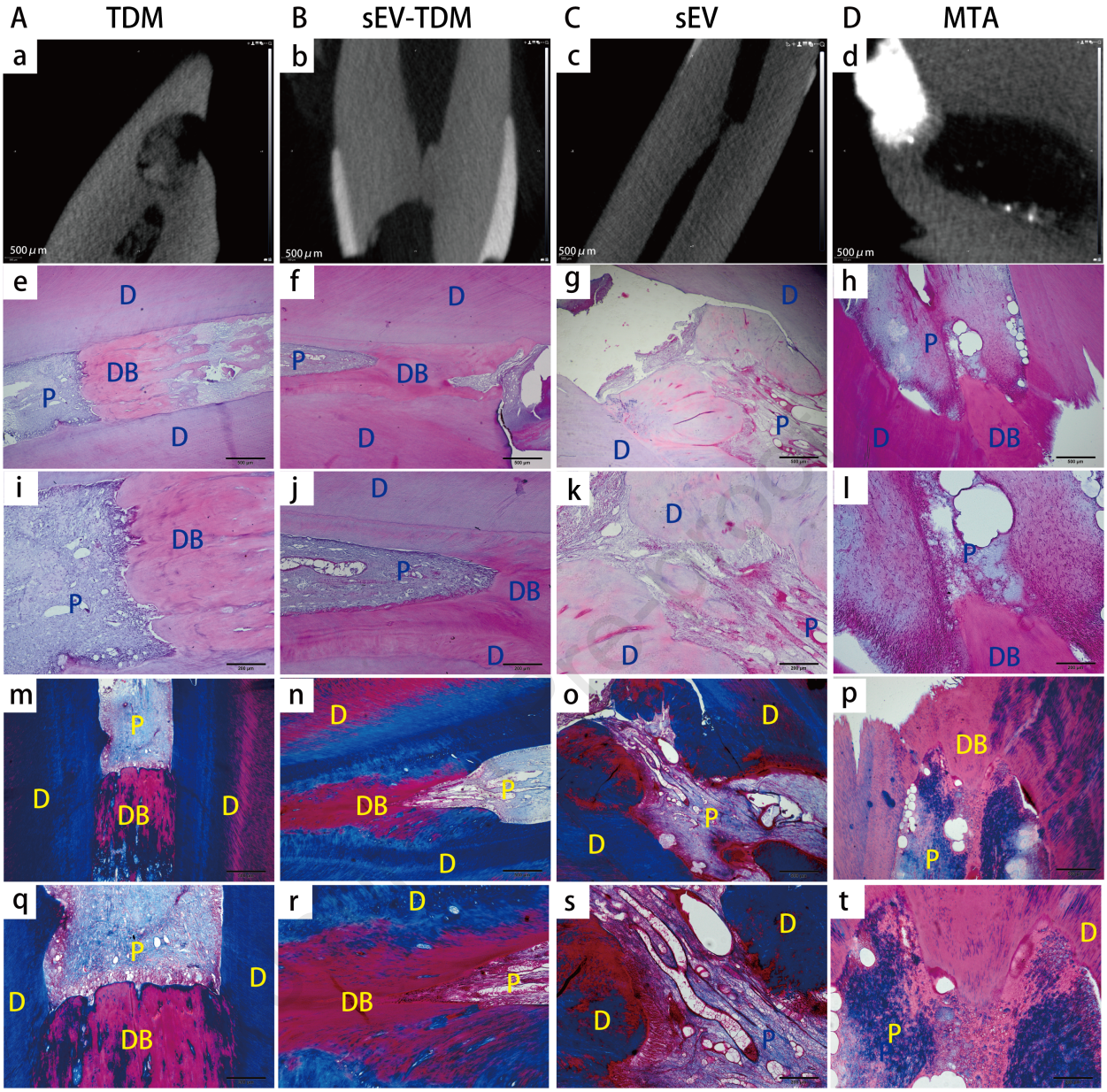
A TDM
B sEV-TDM
C sEV
D MTA
a
b
c
d
500 μm
e
f
g
h
i
j
k
l
m
n
o
p
q
r
s
t
D
DB
P

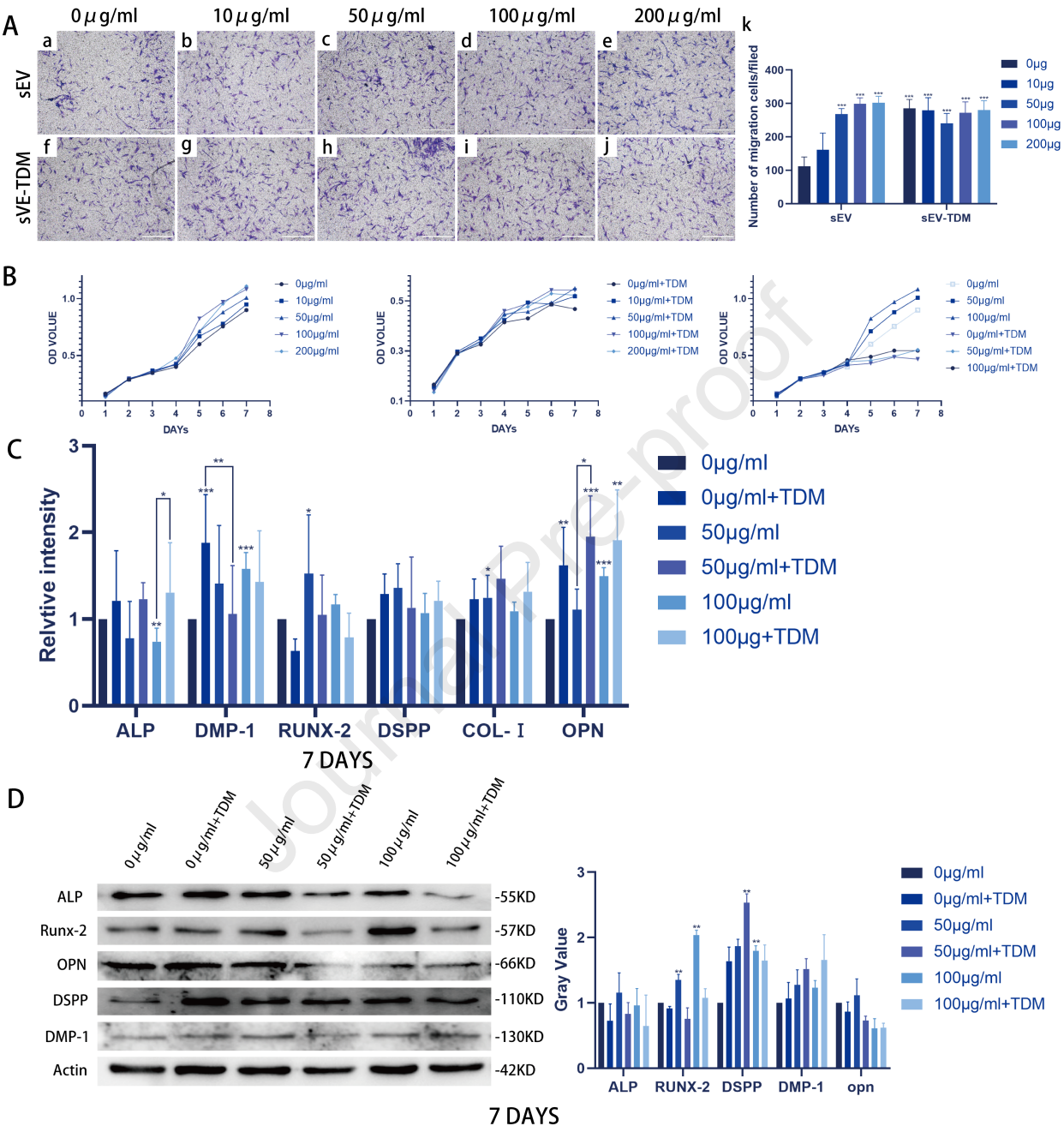

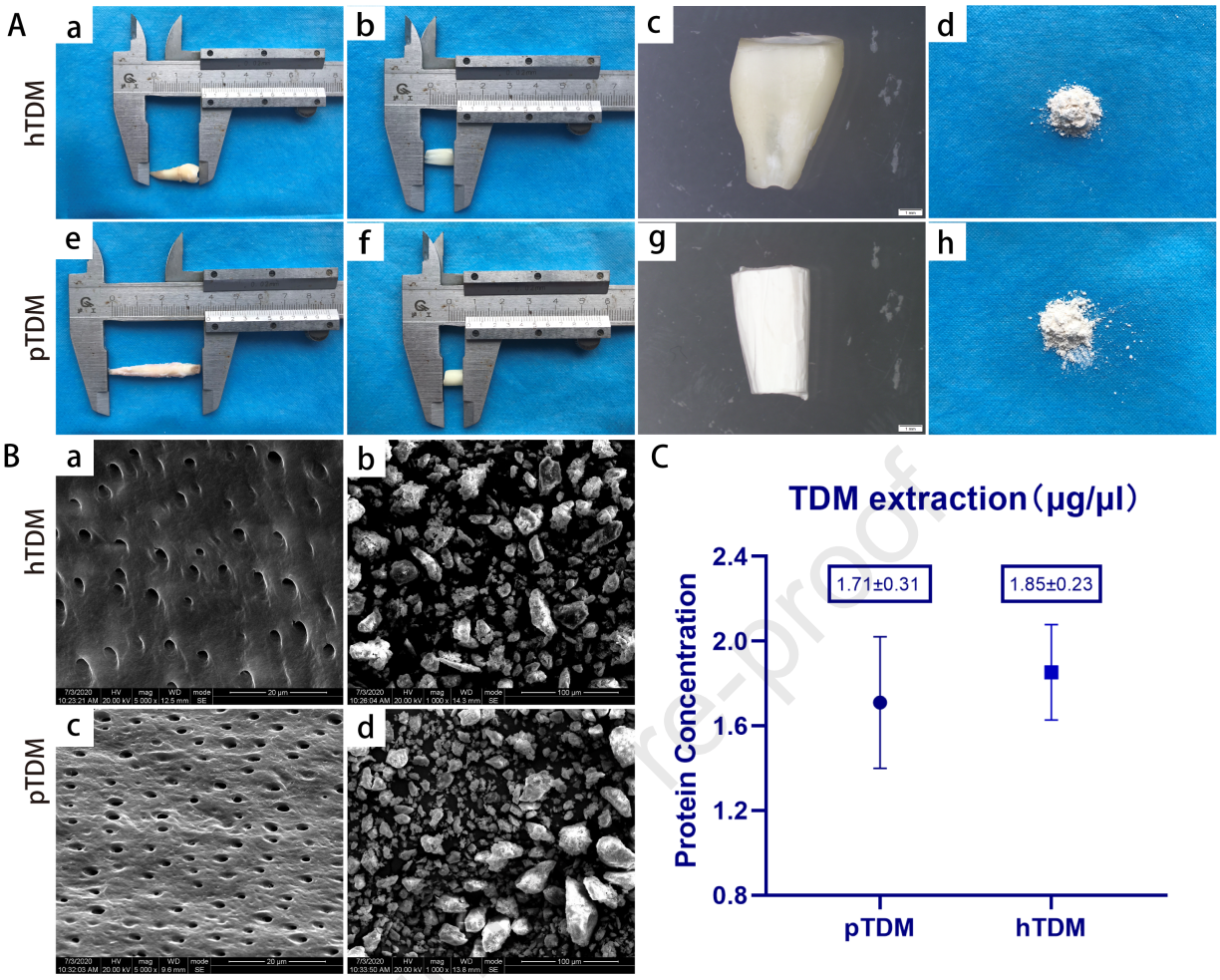

Statement of Clinical Relevance

In this manuscript that informed consent was obtained for experimentation with human subjects. The privacy rights of human subjects must always be observed.